



Nanoarchitectonics for Sensors

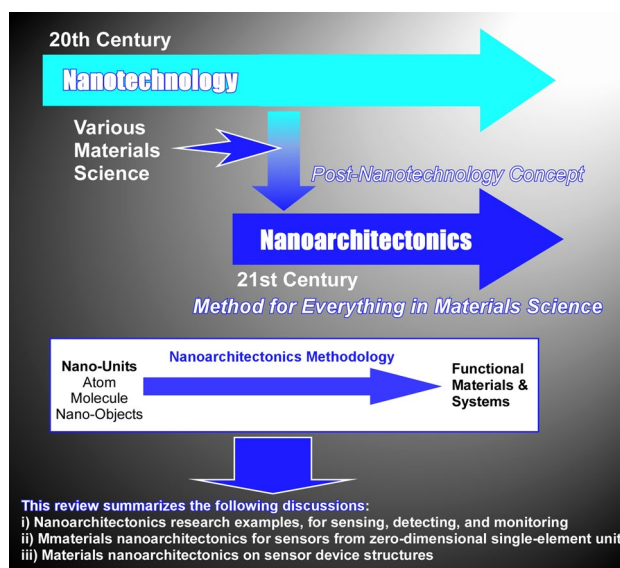
Katsuhiko Ariga^{1,2}

Received: 19 July 2025 / Accepted: 9 October 2025 / Published online: 22 November 2025
© The Author(s) 2025

Abstract

Nanotechnology was founded in the mid-twentieth century, contributing to the development of science and technology at the nano and micro levels. The next step can be achieved through nanoarchitectonics, a post-nanotechnology concept. The nanoarchitectonics approach emphasises the importance of science and technology in the nano world opened up by nanotechnology for synthesising functional materials that actually work. This methodology can also be applied to the development of sensors and related sensing systems. This review will consider the role of nanoarchitectonics in developing such materials by adopting the following methodology. First, several research papers related to sensor research that include ‘nanoarchitectonics’ in the title will be selected. These examples will demonstrate how the concept of nanoarchitectonics is applied to sensor development. The next section will examine the possibility of constructing sensing structures from a materials perspective. This will be demonstrated by showing that diverse and hierarchical sensing structures can be created from fullerenes, which are single-element zero-dimensional materials. The third section will present examples of material structures that can transmit signals and interface with devices. The final section will discuss the future directions and requirements of nanoarchitectonics research for sensor development, based on the information obtained.

Graphical Abstract



Keywords Nanoarchitectonics · Sensor · Fullerene · Device · Interface

✉ Katsuhiko Ariga
ARIGA.Katsuhiko@nims.go.jp

¹ Research Center for Materials Nanoarchitectonics (MANA), National Institute for Materials Science (NIMS), 1-1 Namiki, Tsukuba, Ibaraki 305-0044, Japan

² Graduate School of Frontier Sciences, The University of Tokyo, 5-1-5 Kashiwanoha, Kashiwa, Chiba 277-8561, Japan

1 Introduction

We are developing a variety of functional materials and systems to address issues relating to energy [1–5], environment [6–10] and biomedical issues [11–15]. To develop more precise and efficient systems, we need to create more sophisticated materials and structures. The characteristic of such structures expressing higher functions can actually be seen in many functional systems in living organisms. Therefore, these concepts could be extremely helpful in solving problems related to living organisms. However, this is not limited to the development of biomedicine-related functions. The excellent functional tissue structures involved in processes such as efficient energy conversion — for example, photosynthesis in living systems [16–18] — should be considered a potential solution to the energy problem. Biological functional systems should generally serve as models for the development of artificial functional materials.

There are two reasons why biological systems are capable of performing such advanced functions. Firstly, their structures are designed with great precision. The various functional components are organised in a highly rational manner, resulting in an extremely efficient functional relay, which characteristics can be seen in recent advanced materials [19–21]. Second, their functions are highly dynamic. They can freely perform their functions by dynamically outputting signals and stimuli input from outside the system, as similarly seen in recent advanced systems [22–25]. In other words, biological functional systems are characterised by their ability to perceive external stimuli and function dynamically. One of the goals of modern science may be to develop material systems that mimic this behaviour. More specifically, a typical challenge is developing functional systems, such as sensors, through precise structural control [26–30]. According to this background, the focus of this review will be on the progress of material development for sensing functions.

Considering the above, I would like to provide a brief historical overview of functional material development here. Originally, humans made tools that performed functions by processing materials they obtained. As various chemical fields have developed, humans have become able to create materials not limited to existing ones. Functional development using organic chemistry [31–35], inorganic chemistry [36–39], polymer chemistry [40–44], coordination chemistry [45–49], supramolecular chemistry [50–54], biochemistry [55–59] and other types of material chemistry [60–64] has been actively pursued from the twentieth century to the present day. Throughout this development, a common understanding has emerged. The importance of very fine structures, such as nanostructures, in the expression of functions has been recognised. Even with the same

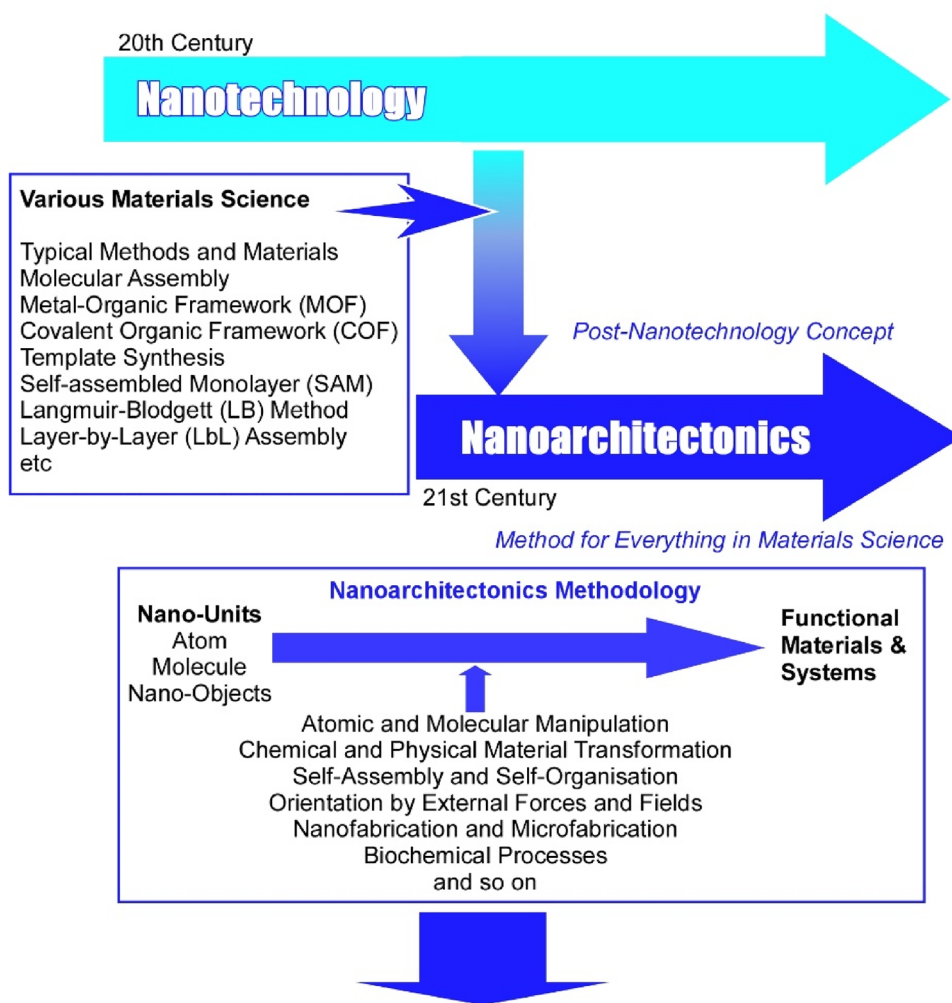
material, new phenomena such as quantum effects [65–68] can be observed by controlling the size at the nanometre scale. Furthermore, when it comes to expressing efficient functions through ingenious molecular and nano-level arrangements [69–71], the contribution of the nanostructure is as important as the intrinsic properties of the material.

Accordingly, technologies for evaluating nanostructures and sciences for creating them are developing. The observation [72–75], manipulation [76–79] and evaluation [80–82] of atoms, molecules and similar microscopic structures and spaces are being actively researched. The synthesis of such nanostructures and materials containing nanostructures is also being widely researched. In addition to fabrication techniques for fine structures using microfabrication and nanofabrication, various chemical processes are also employed. These include creating molecular assembly structures using supramolecular chemistry [83–87], creating metal–organic frameworks (MOFs) [88–91] using coordination chemistry, creating covalent organic frameworks (COFs) [92–95] using polymer chemistry, synthesising mesoporous materials using template synthesis [96–99], and creating self-assembled monolayers (SAMs) [100–103], Langmuir–Blodgett (LB) [104–108] method and layer-by-layer (LbL) assembly [109–112] using interface science.

While these individual developments are important, the concepts that integrate them are equally significant. Such concepts influence major research and development trends. Nanotechnology is a prime example of this. Richard Feynman founded nanotechnology in the mid-twentieth century [113, 114]. Although nanotechnology is a very general concept, it has contributed to the development of science and technology at nano and micro levels. The next step is to develop a concept that utilises the nano-level science and technology revealed by nanotechnology to create functional materials. This is achieved through nanoarchitectonics, a post-nanotechnology concept (Fig. 1) [115]. It was proposed by Masakazu Aono at the beginning of the twenty-first century [116, 117]. It is a methodology that builds functional materials from nano units (atoms, molecules and nanomaterials). This characteristic can also be seen in the aforementioned supramolecular chemistry [118]. Nanoarchitectonics is a concept that integrates them. In other words, it is a broad concept that encompasses nanotechnology and other fields of materials science [119, 120]. The idea is to emphasise the importance of science and technology in the nano world opened up by nanotechnology for the synthesis of functional materials that actually work.

Nanoarchitectonics is an integrated concept. The methodology therefore incorporates various methods, techniques and concepts developed thus far for the creation of functional materials. These materials are constructed by selecting and combining atomic and molecular manipulation, chemical

Fig. 1 History and outline of the nanoarchitectonics concept that encompasses nanotechnology and other fields of materials science with subjects of this review article, nanoarchitectonics for sensors



This review summarizes the following discussions:

- i) Nanoarchitectonics research examples, for sensing, detecting, and monitoring
- ii) Materials nanoarchitectonics for sensors from zero-dimensional single-element unit
- iii) Materials nanoarchitectonics on sensor device structures

and physical material transformation, self-assembly and self-organisation, orientation by external forces and fields, nanofabrication and microfabrication, and biochemical processes [121]. These methods are often used in combination, resulting in a greater likelihood of obtaining asymmetric and hierarchical structures in nanoarchitectonics [122] than in single self-assembly processes. Additionally, nanoarchitectonics as a methodology is not limited to specific materials or applications, making it applicable to a wide range of subjects. Papers with the title ‘nanoarchitectonics’ alone are widely used in many fields, ranging from basic research in physics [123–125], chemistry [126–128], and biochemistry [129–131] to applications in energy [132–135], the environment [136–138], and biomedical targets [139–141]. As all materials are originally made of atoms and molecules, the nanoarchitectonics methodology, which builds materials

from these components, may be applicable to the creation of all materials. While super unification theory is the theory of everything in physics [142], nanoarchitectonics could be considered the method for everything in materials science [143–145]. Even if it is not explicitly referred to as nanoarchitectonics, there are numerous examples of research that can be considered to be based on this approach. Rather than being limited to specific research, nanoarchitectonics indicates the overall flow of research, as does nanotechnology. Building on nanotechnology, nanoarchitectonics indicates the research trend of developing functional materials with nanoscale properties.

The nanoarchitectonics methodology for developing functional materials can also be applied to developing sensors and related sensing systems [146–148]. These systems and their constituent functional materials can selectively

recognise external molecules or signals and output them as useful signals. It is therefore essential to design and synthesise specific structures to identify molecules or signals and construct rational arrangements to transmit signals efficiently. The construction of such structures with nano-level precision is the primary focus of nanoarchitectonics. Therefore, the development of sensors and sensing systems is an ideal application of nanoarchitectonics. In this review, I will consider the role of nanoarchitectonics in developing sensors and related functional materials.

Finally, I would like to introduce the methodology employed in this review. Examining the trend in the number of papers with the title ‘nanoarchitectonics’, it is clear that research in this field has grown dramatically in recent years. In other words, the application of the nanoarchitectonics concept is a recent development and far from complete. Therefore, this review will adopt the following methodology. First, several research papers related to sensor research that include ‘nanoarchitectonics’ in the title will be selected in the section following this introduction. These examples will demonstrate how the concept of nanoarchitectonics is applied to sensor development. The next two sections will narrow the focus to explore the potential contribution of nanoarchitectonics to the development of sensor functional materials. First, the possibility of constructing sensing structures will be examined from a materials perspective. To demonstrate this, it will be shown that diverse and hierarchical sensing structures created from fullerenes (C_{60} , C_{70}), which are single-element zero-dimensional materials, is examined. The next section will present examples of materials structures that can transmit signals and interface with devices. This review summarises the following discussions: i) nanoarchitectonics research examples, for sensing, detecting, and monitoring, ii) materials nanoarchitectonics for sensors from zero-dimensional single-element unit, fullerene, iii) materials nanoarchitectonics on sensor device structures. Based on this information, the final section discusses the future directions and requirements of nanoarchitectonics research for sensor development.

2 Nanoarchitectonics Research Examples, for Sensing, Detecting, and Monitoring

This section will examine how nanoarchitectonics has spread to the field of sensors. The applied methodology will select and briefly introduce several papers related to sensing, detection and monitoring which include the term ‘nanoarchitectonics’ in the title.

The concept of nanoarchitectonics involves arranging and organising molecules to improve sensing behaviour. For example, Fang and his colleagues published a paper titled ‘Film Nanoarchitectonics of Pillar[5]arene for High-Performance Fluorescent Sensing: A Proof-of-Concept Study’ (Fig. 2) [149]. In this study, they present a pillar[5]arene-based nanofilm that is sensitive, fluorescent, free-standing and uniform with tunable thickness. This nanofilm is prepared via dynamic condensation at the air/DMSO interface using an acyl-hydrazine derivative of pillar[5]arene and triformyl-benzene. This nanofilm ensures the spatial and electronic separation of immobilised fluorophores and avoids aggregation-induced quenching in the film state. To demonstrate this concept, they developed a formic acid fluorescent sensing film using a 4-azetidino-1,8-naphthalimide derivative of cholesterol as a fluorescent probe. This film was shown to respond sensitively, rapidly and selectively to formic acid in air. The nanoarchitectonics of the fluorescent probe in the film may be an efficient method for developing fluorescent sensing films.

The aggregation-induced emission enhancement of metal nanoclusters is an attractive mechanism for creating more sensitive sensing systems. However, this is not always straightforward, and nanoarchitectonics-based design is essential. In the paper, ‘Supraparticle Nanoarchitectonics with Bright Gold Nanoclusters Induced by Host–Guest Recognition for Volatile Amine and Meat Freshness Detection’, Peng et al. employed a hybrid supraparticle approach involving the combination of 6-aza-2-thiothymine-capped gold nanoclusters and cucurbit[n]uril (CB[n], $n=7$ and 8) (Fig. 3) [150]. Through host–guest recognition between the

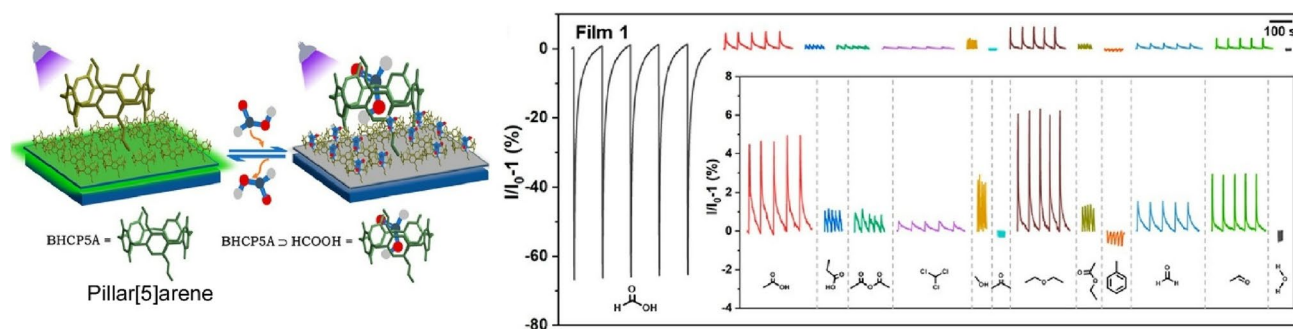


Fig. 2 A pillar[5]arene-based nanofilm with spatial and electronic separation of immobilised fluorophores resulting in sensitively, rapidly and selectively to formic acid in air. Responses to prove selective detection

of formic acid are shown in right side. Reprinted with permission from Ref. 149 Copyright 2021 American Chemical Society

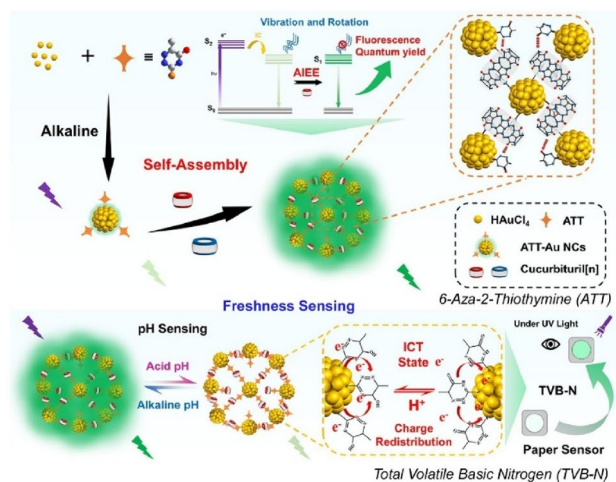


Fig. 3 A hybrid supraparticle approach involving the combination of 6-aza-2-thiothymine-capped gold nanoclusters and cucurbit[n]uril responding sensitively and reversibly to changes in environmental pH as a fluorescent turn-on sensor applicable for monitoring meat freshness. Reprinted with permission from Ref. 150 Copyright 2025 American Chemical Society

CB[n] and 6-aza-2-thiothymine ligands, the weakly fluorescent, unmodified gold nanoclusters assembled into large supraparticles that exhibited a 15-fold increase in fluorescence with a quantum yield of 52%. Due to the protonation reaction of the 6-aza-2-thiothymine ligand, the system can respond sensitively and reversibly to changes in environmental pH. The researchers also developed a fluorescent turn-on sensor and successfully applied it to monitoring meat freshness. Furthermore, due to its customisable surface functional groups, it has the potential to be used in fluorescent imaging, immunoassay labelling and fluorescent hazard sensing.

Nanoarchitectonics, which uses various nanomaterials as components, can be employed to develop sensing systems and the supporting systems. For instance, mechanically flexible micro-supercapacitors could complement or replace

microbatteries in portable biomonitoring devices. Attempts to fabricate these using nanoarchitectonics have been reported. In a paper titled ‘Laser-Induced MXene-Functionalized Graphene Nanoarchitectonics-Based Microsupercapacitor for Health Monitoring Application’, Pumera and colleagues developed a high-energy-density micro-supercapacitor integrated with a force sensor using a picosecond pulsed laser (Fig. 4) [151]. This can be used to monitor the radial artery pulse in the human body. In the material created by this method, oxide nanoparticles derived from laser-induced MXene ($\text{Ti}_3\text{C}_2\text{T}_x$) are uniformly attached to laser-induced graphene, which serves as the active electrode material of the micro-supercapacitor. This hybrid micro-supercapacitor exhibits excellent properties, including high mechanical flexibility, durability, ultra-high energy density, superior capacitance and a long cycle life. As proof of concept, force-sensitive detectors driven by flexibly linked micro-supercapacitors in series were attached to a human wrist to monitor the pulse. Micro-supercapacitors can be connected in series or in parallel to power various LEDs and digital watches, meeting the energy and power requirements of portable electronic devices. They will also be useful for extracting energy more efficiently from solar, thermal and mechanical sources.

Designing material structures using nanoarchitectonics is useful for developing sensing systems for a variety of applications. For example, there is a high demand for the detection of hazardous gases. Real-time gas sensors that can simultaneously detect multiple gases with high sensitivity and selectivity are particularly essential. In the paper, ‘Interfacial Engineering Facilitates Real-Time Detection of Dual Hazardous Gases at ppb Levels via Single-Step Hydrothermal Nanoarchitectonics of Self-Assembled PbSnS/SnO₂ Heterostructures’, Huang, Wu and their colleagues successfully fabricated a thin-film sensor based on PbSnS/SnO₂ heterostructures. They used this sensor to detect two hazardous oxidising gases at room temperature in real time (Fig. 5)

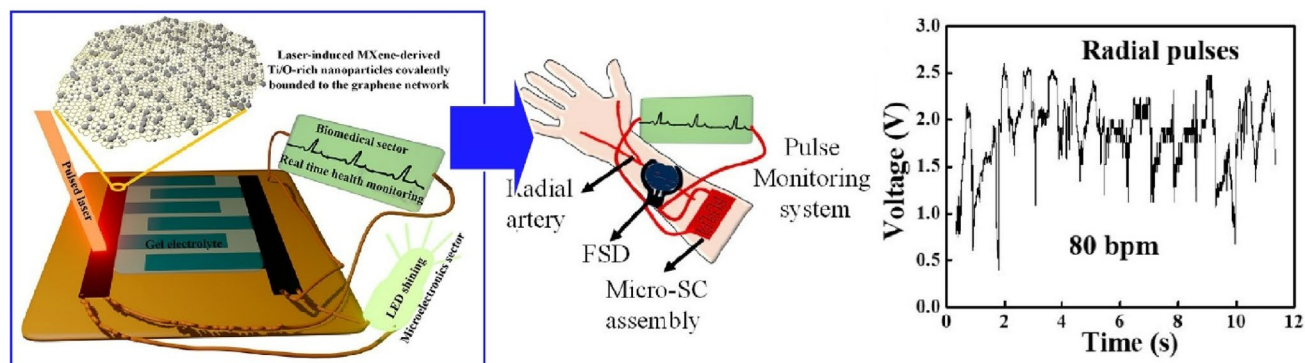


Fig. 4 A high-energy-density micro-supercapacitor integrated with a force sensor using oxide nanoparticles derived from laser-induced MXene ($\text{Ti}_3\text{C}_2\text{T}_x$) used on a human wrist to monitor the pulse. Actual

response is shown in right-hand side. Reproduced under terms of the CC-BY license from Ref. 151, 2023 American Chemical Society

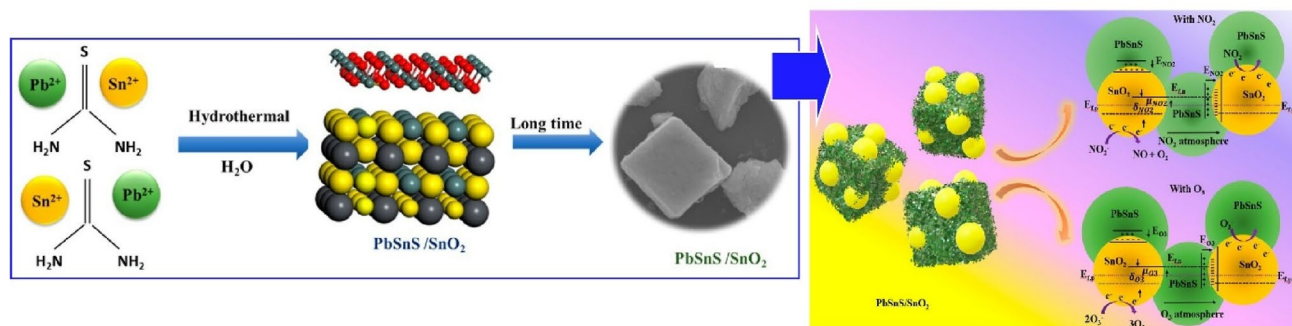


Fig. 5 A thin-film sensor based on PbSnS/SnO₂ heterostructures showing ppb-level limits of detection for NO₂ and O₃ gases. Possible mechanisms for detection are depicted in right part. Reproduced under terms of the CC-BY license from Ref. 152, 2025 American Chemical Society

[152]. In this study, the PbSnS/SnO₂ heterostructures were fabricated using a one-step hydrothermal synthesis method. The heterostructures were drop-cast onto a fork-shaped electrode and dried on a heating plate at 80 °C to fabricate a sensor device. The sensor showed ppb-level limits of detection for NO₂ and O₃ gases. This can be adequately explained by the band diagram. Accumulation regions appear along the grain boundaries of the heterojunction. The potential variations across the junction play an important role in modulating the material's conductive properties. NO₂ molecules absorb electrons from the surrounding atmosphere and transfer them to the PbSnS/SnO₂ after interacting with oxygen species. Conversely, the highly oxidizing O₃ gas acquires electrons from the surrounding atmosphere, ionises them and adsorbs onto the oxygen species present on the PbSnS/SnO₂ surface. O₂ donates electrons to the PbSnS/SnO₂ material. These findings demonstrate the effectiveness of PbSnS/SnO₂ heterostructures fabricated using nanoarchitectonics for gas sensing applications. Furthermore, they may contribute to a better understanding of the fundamental principles that govern the gas adsorption process.

Medical sensing is an essential application. Ciprofloxacin, for example, is a fluoroquinolone antibiotic prescribed to patients infected with Gram-positive and Gram-negative aerobic pathogens. However, measuring the concentration of ciprofloxacin in urine samples specifically is challenging due to interference from uric acid. In the report, 'Nanoarchitectonics of Polyaniline-Poly(Vinyl Pyrrolidone)-Graphene Composite for the Electrochemical Sensing of Ciprofloxacin and Uric Acid', Perumal, Kumar, Lee and their colleagues fabricated a polyaniline-poly(vinyl pyrrolidone)-graphene composite electrode using nanoarchitectonics to measure ciprofloxacin and uric acid simultaneously in human urine samples (Fig. 6) [153]. Graphite-polyaniline was prepared by the oxidative polymerisation of aniline in the presence of graphene. Vinyl pyrrolidone was then polymerised on the surface via free radical polymerisation. Using this composite electrode confirmed that similar concentrations of ciprofloxacin and uric acid in human urine samples could be

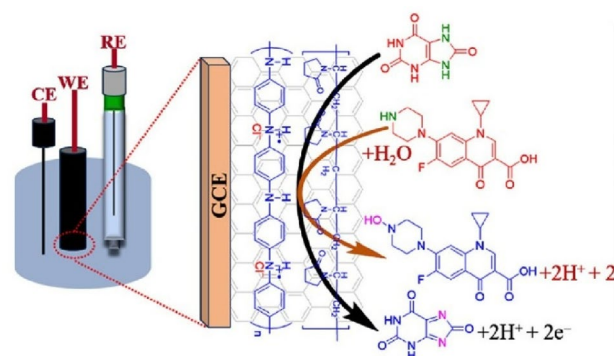


Fig. 6 A polyaniline-poly(vinyl pyrrolidone)-graphene composite electrode using nanoarchitectonics to measure ciprofloxacin and uric acid simultaneously in human urine samples. Reprinted with permission from Ref. 153 Copyright 2025 Elsevier

detected simultaneously with excellent sensitivity and a low detection limit, respectively. The ability of the composite electrode to detect both substances simultaneously is promising for practical applications.

The development of a portable, light-assisted, self-powered sensing platform with high sensitivity and selectivity is attractive. In their paper, 'Photo-Assisted Zn-Air Battery Promoted Self-Powered Sensor for Selective and Sensitive Detection of Antioxidant Gallic acid Based on Z-Scheme Nanoarchitectonics with Heterojunction AgBr/CuBi₂O₄', Du, Chen and their colleagues developed a self-powered electrochemical sensor. They used a light-assisted Zn-air battery as an energy conversion device to detect gallic acid with high sensitivity (Fig. 7) [154]. Introducing visible light into the Zn-air battery system improved the output signal of the novel self-powered sensor. Photoelectric conversion efficiency improved due to the separation of electron-hole pairs promoted by the Z-type heterojunction. The light-assisted oxygen reduction reaction (ORR) process was promoted, thereby improving the output signal of the sensor. The selectivity of the fabricated sensor was realised due to the chelating effect between AgBr/CuBi₂O₄ and gallic acid.

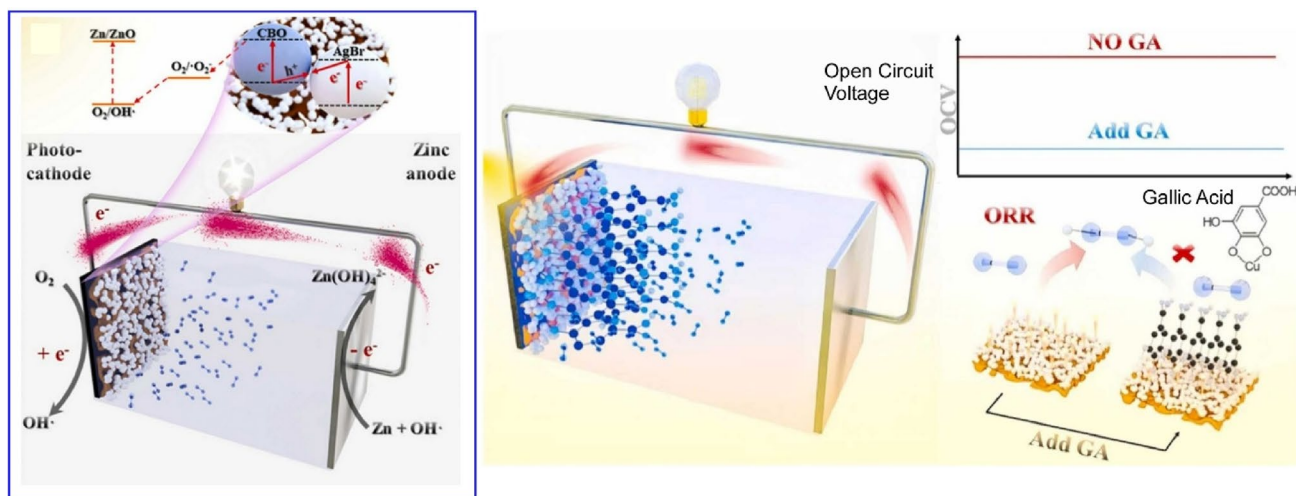


Fig. 7 An energy conversion device to detect gallic acid with high sensitivity in which photoelectric conversion efficiency can be improved due to the separation of electron–hole pairs promoted by the Z-type heterojunction. The light-assisted oxygen reduction reaction (ORR)

process was promoted, thereby improving the output signal of the sensor. The selectivity of the fabricated sensor was realised due to the chelating effect between AgBr/CuBi₂O₄ and gallic acid. Reprinted with permission from Ref. 154 Copyright 2023 Elsevier

Synthesis and Electrochemical Deposition of Flexible Mesoporous Metallic Gold

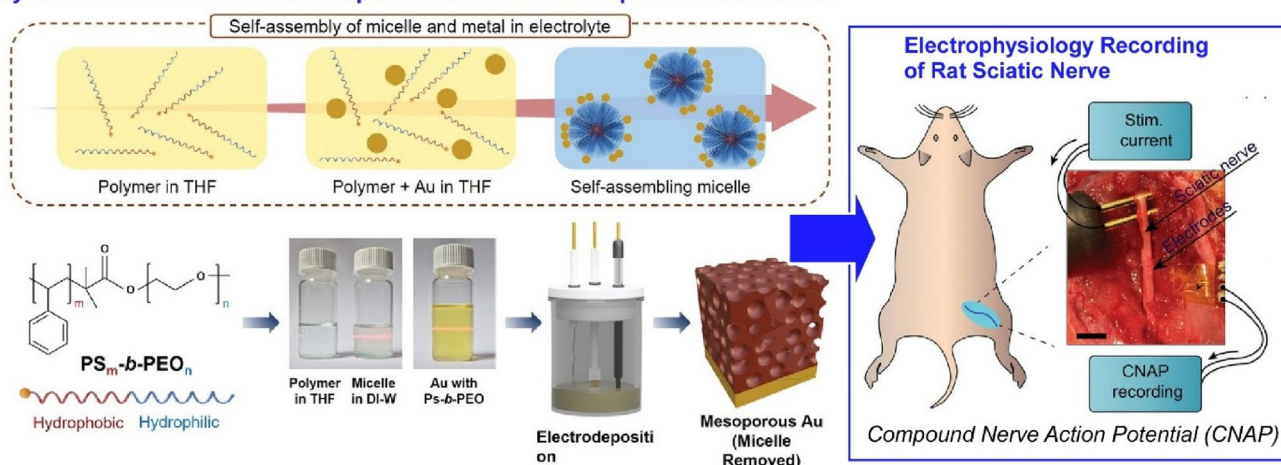


Fig. 8 Combination of bottom-up mesoporous fabrication techniques with top-down microlithography processes to create flexible, low-impedance mesoporous gold electrodes for use in biosensing and bio-

implant applications as connected to the sciatic nerve stimulation site to monitor electrophysiological recording performance. Reproduced under terms of the CC-BY license from Ref. 155, 2023 Wiley–VCH

Sensing systems can also be constructed to monitor physiological activities. In the paper, ‘Flexible Nanoarchitectonics for Biosensing and Physiological Monitoring Applications’, Ashok et al. combined bottom-up mesoporous fabrication techniques with top-down microlithography processes to create flexible, low-impedance mesoporous gold electrodes for use in biosensing and bioimplant applications (Fig. 8) [155]. The large surface area of the mesoporous network enables high current density transmission in standard electrolytes. Connecting all active electrodes to a common working electrode terminal enables the selective and simultaneous deposition of mesoporous structures onto a seed layer. This results in a monitoring system that utilises

selective electrochemical integration on pre-patterned microstructures. The detection of compound nerve action potentials in rat peripheral nerves was demonstrated. The flexible mesoporous electrodes were connected to the sciatic nerve stimulation site to monitor electrophysiological recording performance. These types of material and sensor design can also serve as innovative platforms for implantable electronics and biological sensing applications.

In the study, ‘Organic–Inorganic Cascade-Sensitized Nanoarchitectonics for Photoelectrochemical Detection of β 2-MG Protein’, Yuan, Chai and their colleagues fabricated a novel photoelectrochemical immunoassay. This is based on organic–inorganic BiVO₄/rGO/FeOOH/C dots, which

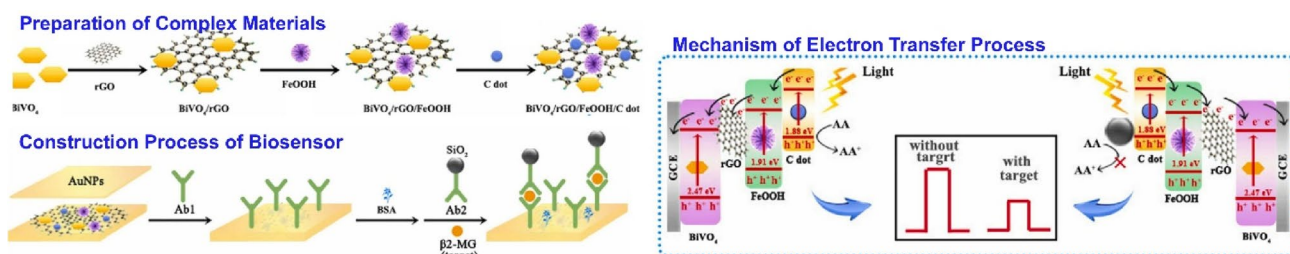


Fig. 9 An organic–inorganic BiVO₄/rGO/FeOOH/C dot hybrid, which act as a cascade-sensitized photoactive material for the ultrasensitive detection of β2-MG protein. Mechanisms of electron transfer processes

for detection are represented in right hand side figure. Reprinted with permission from Ref. 156 Copyright 2024 Elsevier

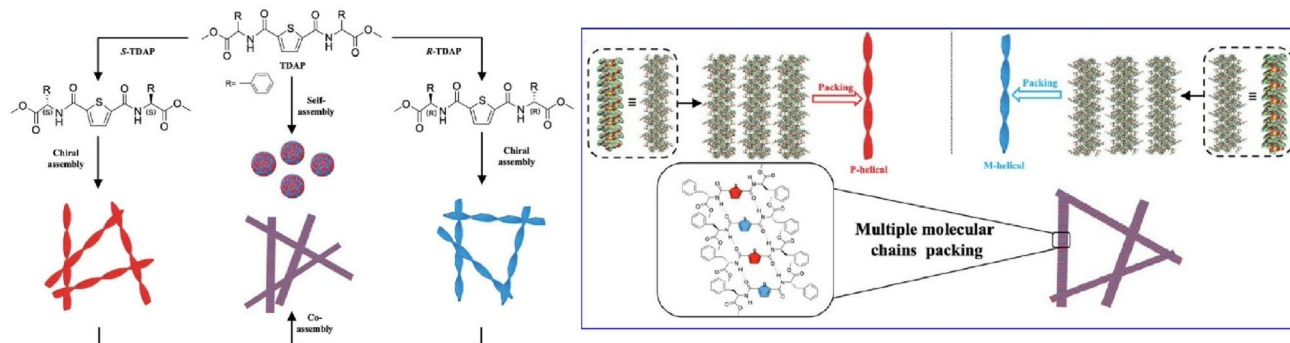


Fig. 10 Molecular detection of the achiral compound melamine as achieved through the emergence of helicity and inversion in a supramolecular system containing COOH groups. Plausible structural

motifs are shown in right. Reprinted with permission from Ref. 157 Copyright 2022 Wiley–VCH

act as a cascade-sensitized photoactive material. This allows for the ultrasensitive detection of β2-MG protein (Fig. 9) [156]. This composite material combines the advantages of the high light absorption efficiency of organic materials with the fast electric carrier mobility of inorganic materials. This composite material with well-matched energy levels can mediate multi-electron transport, thereby effectively promoting electron transfer and improving charge separation to achieve excellent photocurrent. In other words, this photoelectrochemical biosensor perfectly exemplifies the organic–inorganic cascade sensitisation strategy. When the target analyte β2-MG protein, with gold nanoparticles and antibody 1 (Ab1) attached, comes into contact with the surface, a sandwich immunoreaction is triggered to capture SiO₂-labelled antibody 2. Due to the electrical inertness and optical coverage effect of SiO₂, the signal of the highly sensitive detection target is significantly reduced. Consequently, the β2-MG protein can be detected with high sensitivity at a low limit of detection. This cascade sensitisation strategy for highly sensitive detection is expected to have a wide range of applications in disease monitoring.

Nanoarchitectonics sensing methods include molecular sensing through the formation of structures, such as molecular assemblies. In a study titled ‘Hierarchical Chiral Supramolecular Nanoarchitectonics with Molecular Detection: Helical Structure Controls upon Self-Assembly

and Coassembly’, He and his colleagues investigated the morphological transformation of microspheres into helical supramolecular nanofibres with controllable handedness (Fig. 10) [157]. Molecular detection of the achiral compound melamine was achieved through the emergence of helicity and inversion in a supramolecular system containing COOH groups. First, uniform microspheres undergo self-assembly. When chiral enantiomers are introduced into the supramolecular system, nanofibres with P- and M-helicity are formed. Furthermore, the coexistence of R- and S-isomers results in the formation of racemic microspheres that lack chiral properties. In the case of enantiomers, these molecules arrange themselves into molecular chains and assemble via hydrogen bond interactions formed between the carbonyl (C=O) and secondary amine groups, with moderate interaction distances. The different migration directions of the hydrogen bonds induce different molecular arrangements and packing of the molecular chains in different conformations. After the introduction of COOH groups, Interaction with melamine induces a morphological transformation involving the appearance and inversion of helicity. This allowed the detection of melamine.

Biomolecular nanoarchitectonics is also being used to develop sensing materials. In a paper titled ‘Nanoarchitectonics of Small Molecule and DNA for Ultrasensitive Detection of Mercury’, Govindaraju et al. demonstrated the

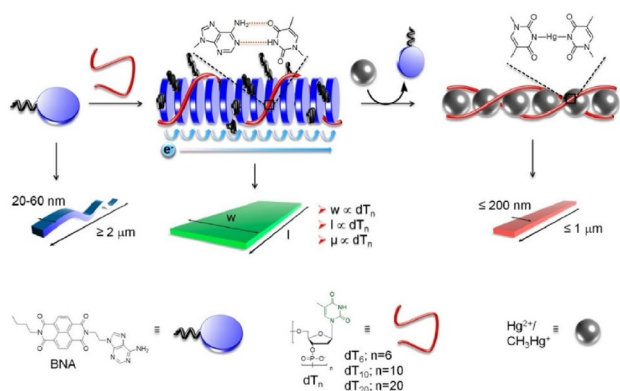
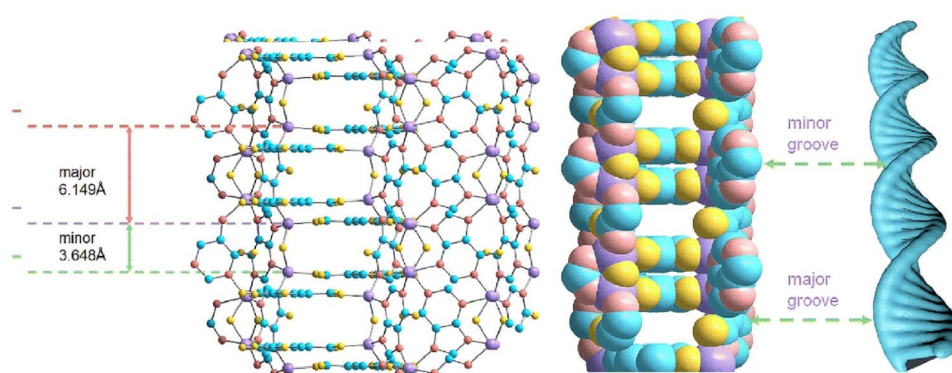


Fig. 11 Ultrasensitive detection of mercury by utilising the intrinsic property of dT_n for complementary base pairing with adenine (A)-linked stacks of small-molecule organic semiconductors (BNA) as achieved through chiroptical signal changes and conductivity in response to mercury ions in water. Reprinted with permission from Ref. 158 Copyright 2016 American Chemical Society

ultrasensitive detection of mercury by utilising the intrinsic property of dT_n for complementary base pairing with adenine (A)-linked stacks of small-molecule organic semiconductors (BNA) (Fig. 11) [158]. The DNA system forms a two-dimensional sheet whose size depends on the length of the dT_n sequence. This nanoarchitecture rapidly converts the BNA- dT_n co-assembly into a metallic DNA duplex [$dT\text{-Hg}\text{-}dT$] $_n$ through mercury-thymine interactions. Subnanomolar mercury detection sensitivity was achieved through chiroptical signal changes and conductivity in response to mercury ions (inorganic and organometallic forms) in water.

Nanoarchitectonics that mimic biomolecules can also be used for sensing purposes. Biomimetic chiral metal–organic frameworks (BioMOFs) can recognise chiral molecules that mimic biological functional systems. In a paper titled ‘Adaptive Host–Guest Chiral Recognition in Nanoarchitectonics with Biomimetic MOF Mimicking DNA’, Niu, Wang and their colleagues successfully synthesised a biomimetic metal–organic framework (MOF) called $ZnBTCH_x$ (BTC = 1,3,5-benzenetricarboxylic acid, Hx = hypoxanthine) that has periodic minor and major grooves resembling the double helix structure of DNA (Fig. 12) [159].

Fig. 12 A biomimetic metal–organic framework (MOF) called $ZnBTCH_x$ (BTC = 1,3,5-benzenetricarboxylic acid, Hx = hypoxanthine) that has periodic minor and major grooves resembling the double helix structure of DNA, enabling the specific recognition of chiral guests. Reprinted with permission from Ref. 159 Copyright 2023 Royal Society of Chemistry

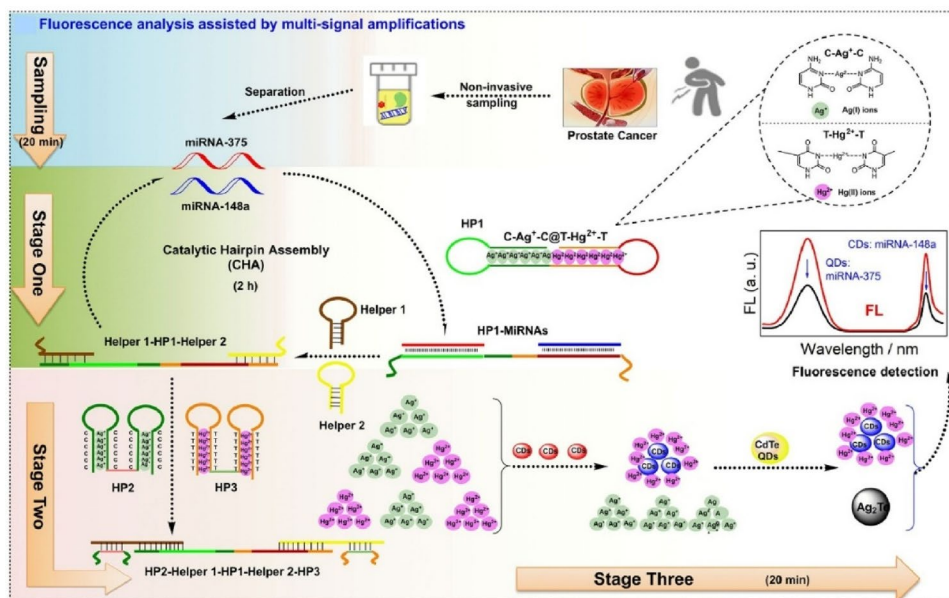


The local shape contained within this structure enables the specific recognition of chiral guests. The result is a bio-inspired chiral MOF with periodic minor and major grooves that resemble the double helix structure of DNA. The major groove of $ZnBTCH_x$'s local shape can undergo strong $\pi\text{-}\pi$ interactions with chiral guests and generate hydrogen bonds with the minor groove. For instance, L- and D-tryptophan (L-/D-Trp) enter the major groove of $ZnBTCH_x$ as chiral guests and bind to the chiral host BTC via hydrogen bonds. This study may provide a new structural design guide for electrochemical chiral recognition in cutting-edge biomedical applications.

Nanoarchitectonics-based material design can also be employed in more practical medical applications. In their paper, ‘Nanoarchitectonics-Assisted Simultaneous Fluorescence Detection of Urinary Dual miRNAs for Noninvasive Diagnosis of Prostate Cancer’, Chen et al. reported a fluorescent strategy for the homogeneous and simultaneous analysis of miR-375 and miR-148a in urine (Fig. 13) [160]. With the aim of achieving an early diagnosis of prostate cancer, the researchers used a dumbbell-shaped DNA containing C– Ag^+ –C and T– Hg^{2+} –T structures, as well as four hairpin DNA strands, to configure a cascade-type response amplification. When combined with fluorescent CdTe quantum dots and carbon dots that are selectively quenched by Ag^+ and Hg^{2+} , highly sensitive detection is achieved simultaneously. Further evaluation was performed on 45 clinical urine samples, including those from patients with prostate cancer and other conditions. The results were consistent with those of clinical polymerase chain reaction (PCR) kits, ultrasound scans and pathological findings. This approach establishes a simple, sensitive nanoarchitectonics strategy for simultaneously analysing miRNAs 375 and 148a in urine.

This section focuses on examples of sensors and sensing functions from recent papers that include the term ‘nanoarchitectonics’ in the title. The examples shown here are not exhaustive, but demonstrate the wide variety of applications. For instance, pillar[5]arene-based nanofilms intended for the production of highly sensitive fluorescent sensing films, and the aggregation-induced emission enhancement

Fig. 13 A fluorescent strategy for the homogeneous and simultaneous analysis of miR-375 and miR-148a in urine, using a dumbbell-shaped DNA containing C–Ag⁺–C and T–Hg²⁺–T structures, as well as four hairpin DNA strands, to configure a cascade-type response amplification. This approach establishes a simple, sensitive nanoarchitectonics strategy for simultaneously analysing miRNAs in urine. Reprinted with permission from Ref. 160 Copyright 2023 American Chemical Society



of metal nanoclusters, are presented as instances of sensors that utilise material structure. Other examples include a real-time thin-film sensor for harmful oxidising gases based on a PbSnS/SnO₂ heterostructure; simultaneous measurement of biomolecules using composite electrodes; and photoelectrochemical immunoassays based on cascade-sensitised photoactive materials. Supramolecular structures and the unique structures of biomolecules are particularly prevalent in sensing applications. These include the molecular detection of achiral melamine through the emergence of helicity and inversion in supramolecular systems; the ultra-sensitive detection of mercury using the properties of stacks of adenine-bound small-molecule organic semiconductors; the specific recognition of chiral guests by biological chiral metal–organic frameworks with a structure similar to that of DNA; and the homogeneous and simultaneous analysis of microRNA-375 and microRNA-148a in urine through cascade-type response amplification. In addition, examples of peripheral devices that support sensor functions have been developed. These include a self-powered electrochemical sensor that uses a light-assisted zinc-air battery for energy conversion, a micro-supercapacitor with a high energy density that is integrated with a force sensor, and a flexible, low-impedance mesoporous gold electrode that is used for biosensing applications. The materials used and their applications are generally very diverse. A variety of fabrication methods and material chemistries are employed. This reflects the fact that nanoarchitectonics is a fusion of nanotechnology and materials science. A distinctive feature is the strong trend towards developing sensors for more complex targets, such as biomaterials and biological phenomena. Distinguishing a specific molecule from similar molecules, including chiral molecules, in biological systems is not

always easy. A precisely constructed recognition site is necessary. Creating such a recognition structure requires various techniques. Integrating technologies to build functional structures is an area in which nanoarchitectonics excels. Nanoarchitectonics will play an increasingly important role in biosensor development.

3 Materials Nanoarchitectonics for Sensors from Zero-Dimensional Single-Element Unit, Fullerene

The above section examined examples of nanoarchitectonics sensor applications and discussed their breadth and future potential. The next two sections will explore the profound capabilities of sensing structure construction from a material chemistry perspective, as well as new approaches to deriving sensing signals from nanoarchitectonics materials. The first of these will discuss structures constructed by fullerene nanoarchitectonics, demonstrating how diverse recognition structures can be formed from basic building blocks. Fullerenes (mainly C₆₀ and C₇₀) consist of a single element and, from a material perspective, are zero-dimensional objects. Considering the diverse recognition structures constructed from such simple units is crucial to understanding the utility of nanoarchitectonics.

The liquid–liquid interfacial precipitation (LLIP) method is a useful technique for the nanoarchitectonics of various fullerene structures. In this method, fullerene is dissolved in a solvent in which it is soluble. Then, a solvent with low solubility for fullerene is added to cause precipitation at the interface. This method can produce a variety of structures, including rods/tubes [161, 162], planar polygons [163, 164]

and cubic structures [165, 166]. Changing the combination of solvents, the way the solvent is added, or post-processing can also produce hierarchical structures [167, 168]. Such structures are often advantageous for sensing various substances. This section will show some typical examples below.

Bairi et al. fabricated a hierarchical structure consisting of mesoporous C_{70} nanorods with crystalline pore walls that extend from the surface of a C_{70} cube (Fig. 14) [169]. The C_{70} cubes were first formed as highly crystalline, cubic objects using LLIP with a liquid–liquid interface between a C_{70} mesitylene solution and *tert*-butyl alcohol. After washing the C_{70} cubes with isopropanol, C_{70} nanorods grow from their surfaces. Each nanorod also develops mesoporosity on its surface. This hierarchical structure is highly effective as a sensing material in the gas phase due to its large sensing surface area and the ease with which guest molecules can diffuse through the mesoporous structure. These guest molecules can then undergo strong π - π interactions with the sp^2 carbon-rich pore walls of the fullerene. In particular, the nanorod structure acts as π - π sensing antenna, similar to an insect's antennae. This hierarchical structure is an excellent sensing material for gas-phase aromatic solvents. It was immobilised on a quartz crystal microbalance (QCM) substrate to construct a sensing system. When the QCM sensor was exposed to solvent vapour, a very fast and sensitive frequency shift was observed. The magnitude of this frequency shift varied significantly depending on the gas-phase guest molecule present. Notably, the response to aromatic solvent vapours, such as toluene and pyridine, was greater than to aliphatic hydrocarbon vapours, such as cyclohexane and hexane. Despite their similar hydrophobicity and molecular dimensions, a significant difference in frequency shift was observed. This suggests that the structure functions as an excellent sensing antenna that is selective for aromatic guest molecules, favouring strong π - π interactions between the

host and guest. It could therefore serve as a highly selective sensing antenna system for toxic aromatic solvent vapours. However, the specific energetic analysis of π - π interactions and structure-performance correlation laws are not fully developed yet. This further exploration will be done with controlled formation of hierarchical fullerene assemblies.

As shown above, hierarchical structures can be formed by extending one shape from another. Conversely, they can be obtained by drilling holes into a structure of a particular shape. Hsieh et al. reported a new method called 'beaker nanolithography' for constructing hollow fullerene nanostructures (Fig. 15) [170]. This solution-based method involves face-selective chemical etching of fullerene crystals under normal conditions of room temperature and pressure. First, C_{60} fullerene nanorods, C_{60} fullerene nanosheets and C_{70} fullerene cubes were prepared as etching targets using LLIP and related methods. These crystals were then chemically etched by utilising the property of fullerene molecules reacting with ethylenediamine. The etching behaviour exhibited face selectivity according to the shape of the object. For example, in the case of one-dimensional fullerene C_{60} nanorods, selective etching occurred at the ends, resulting in hollow fullerene nanotubes. For two-dimensional C_{60} fullerene nanosheets, etching mainly occurred on the top and bottom surfaces of the sheets, with partial etching at the edges. For the three-dimensional C_{70} fullerene cubes, etching occurred on all faces of the cube to form objects with a gyroid-like morphology. The chemically etched fullerene nanostructures exhibited excellent vapour sensing performance, being selective for acidic guest molecules over aromatic molecules due to the attachment and functionalisation of ethylenediamine. For example, the response of the QCM sensor immobilised with etched hollow fullerene nanotubes to acidic vapours, such as formic acid and acetic acid, was greater than the response to aromatic solvent vapours, such as benzene and toluene. In other words, despite the higher

Fig. 14 A hierarchical structure consisting of mesoporous C_{70} nanorods with crystalline pore walls that extend from the surface of a C_{70} cube. These guest molecules can then undergo strong π - π interactions with the sp^2 carbon-rich pore walls of the fullerene. In particular, the nanorod structure acts as π - π sensing antenna. Reprinted with permission from Ref. 169 Copyright 2016 American Chemical Society

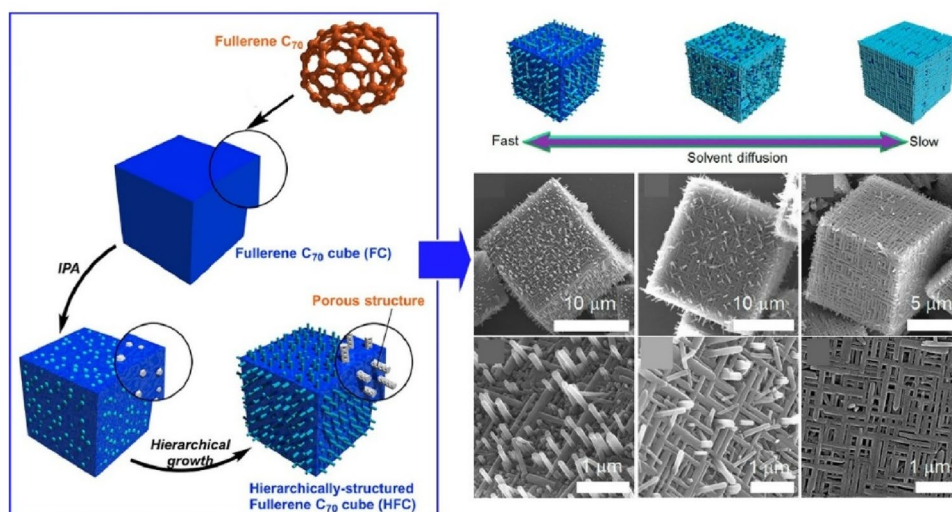


Fig. 15 A ‘beaker nanolithography’ for constructing hollow fullerene nanostructures through face-selective chemical etching of fullerene crystals under normal conditions of room temperature and pressure utilising the property of fullerene molecules reacting with ethylenediamine. Reprinted with permission from Ref. 170 Copyright 2020 Royal Society of Chemistry

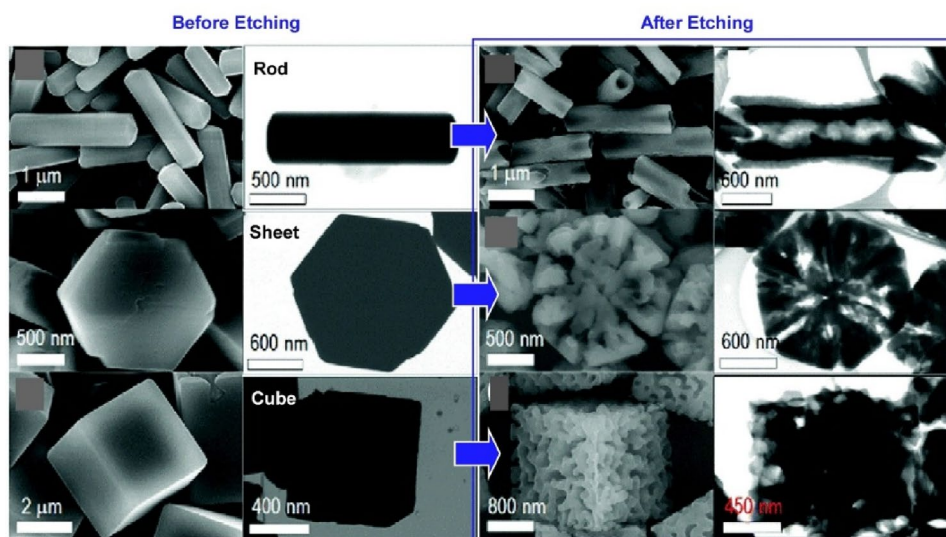
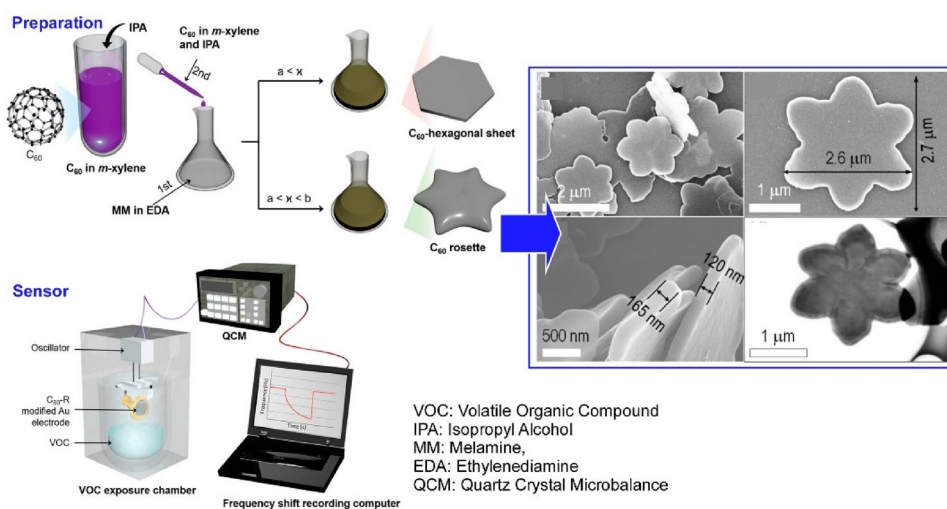


Fig. 16 In situ Reaction method during the self-organisation process of C_{60} molecules in solution, adding melamine and ethylenediamine components to create a new type of fullerene aggregate, a fullerene rosette. The fullerene rosette is a two-dimensional material with an extremely smooth surface and a thickness ranging from 120 to 165 nm. Reproduced under terms of the CC-BY license from Ref. 171, 2022 MDPI



saturated vapour pressure of aromatic vapours, the selectivity for acidic vapours was high. The order of selectivity for all other etched objects was formic acid > acetic acid > propionic acid > phenol > formaldehyde. The large surface area created by etching also improved the sensitivity of the sensor. This ‘beaker nanolithography’ process is simple and scalable, in contrast to the expensive lithography techniques that are usually employed. In addition to developing sensing materials, this technology is expected to be useful for biological and ion sensing, separation processes, energy storage and drug carrier applications.

Carrying out the assembly and reaction processes of fullerenes in parallel enables the creation of objects with specific shapes. Chen et al. used the in situ reaction method during the self-organisation process of C_{60} molecules in solution, adding melamine and ethylenediamine components to create a new type of fullerene aggregate. This regular object has a micron-sized, two-dimensional, amorphous

shape: a fullerene rosette (Fig. 16) [171]. Composed of a six-petal structure, the fullerene rosette is a two-dimensional material with an extremely smooth surface and a thickness ranging from 120 to 165 nm. Analysis results suggested that the melamine/ethylenediamine components strongly interacted with, or were covalently bonded to, the fullerenes in the fullerene rosette. XRD analysis also revealed that the fullerene rosette was amorphous and non-crystalline. A sensor system was prototyped by immobilising the fullerene rosette on the surface of a QCM. As a preliminary result of the hazardous substance sensing requested by society, selective sensing of formic acid was demonstrated. A rapid frequency shift was observed upon exposure to volatile organic compounds, and the frequency returned to nearly the initial state when the solvent vapour was removed from the chamber. This suggests reversible vapour adsorption/desorption. Alternating exposure to and removal of formic acid vapour demonstrated the excellent sensing performance and good

reproducibility of the fullerene rosette-modified QCM sensor. Sensors for formic acid and related compounds are required for air quality monitoring and health diagnostics. The relative simplicity of this methodology could be applicable to more practical sensing systems for a variety of chemical targets, including important volatile organic compounds.

Fabrication is possible not only for individual 2D materials, but also for widely spread 2D sheet-like structures. Ultrathin 2D nanoporous materials, in particular, are important structures for the selective recognition of guest molecules, as they provide enhanced sensitivity and high spatial resolution in sensing applications. Song et al. reported the bottom-up fabrication of a novel, molecularly thin, nitrogen-doped 2D material called fullerphene (Fig. 17) [172]. First, a large-area, molecularly thin, 2D fullerene-ethylenediamine (EDA) film was fabricated by the self-assembly and cross-linking of fullerene and ethylenediamine molecules at the liquid–liquid interface. The formed film could be transferred onto different substrates by a simple scooping procedure. Then, a carbon nanomembrane of fullerphene was produced by carbonisation at 700 °C. This ultrathin, heat-treated 2D carbon film retained its nanofilm morphology following carbonisation. Fullerphene has an ultrafine porous nanostructure that is mainly composed of sp^2 -bonded carbon atoms. The N-doping of fullerphene is dominated by pyrrolic and quaternary nitrogen atoms. These structural features enable the selective and repeatable adsorption and desorption of low-molecular-weight carboxylic acid vapours through non-covalent interactions. In particular, it exhibited high selectivity between acetic acid and formic acid, demonstrating molecular discrimination at the level of a single carbon atom. The large surface area and well-defined, ultrafine pores of fullerphene films are highly beneficial for vapour

adsorption sensing processes based on both acidity and the molecular dimensions of analytes.

Hybrid structures combining fullerene aggregates with other structures can also be created. In a further development in the field of hierarchical composites, which combines coordination and supramolecular chemistry, Bhadra et al. developed a new material: a metal–organic framework (MOF) on a fullerene aggregate (MOFOF) (Fig. 18) [173]. The MOFOF synthesis procedure involves the initial controlled fabrication of the fullerene as a tubular nanostructure (fullerene nanotube), followed by surface functionalisation and surface growth of the MOF (ZIF-67 in this case). MOFOFs can be highly hierarchical composites with properties such as micro- and mesopore channels, interfacial facets and defect sites. These properties lead to potential applications in areas such as gas storage and separation, catalysis, sensing, energy storage and environmental remediation. A QCM sensor modified with MOFOF was tested for its ability to detect vapours. The sensor's detection properties for a wide range of VOCs were observed, with the sensitivity/selectivity order being formic acid > acetic acid > toluene > benzene > cyclohexane > hexane > pyridine > acetone > aniline. Furthermore, integrating other types of MOFs with different fullerene-based nanostructures could result in composite materials with customised functions for various applications, such as catalysis, gas storage, and environmental remediation.

Some research has been conducted into creating material void structures for the selective sensing of particles rather than molecules. A solution-based self-assembly strategy was used to fabricate highly crystalline fullerene C_{70} cubes with open-hole structures in the centre of each face as reported by Bairi et al. (Fig. 19) [174]. These open-hole structures can be intentionally closed by introducing additional C_{70} molecules, and reopened by irradiating them with

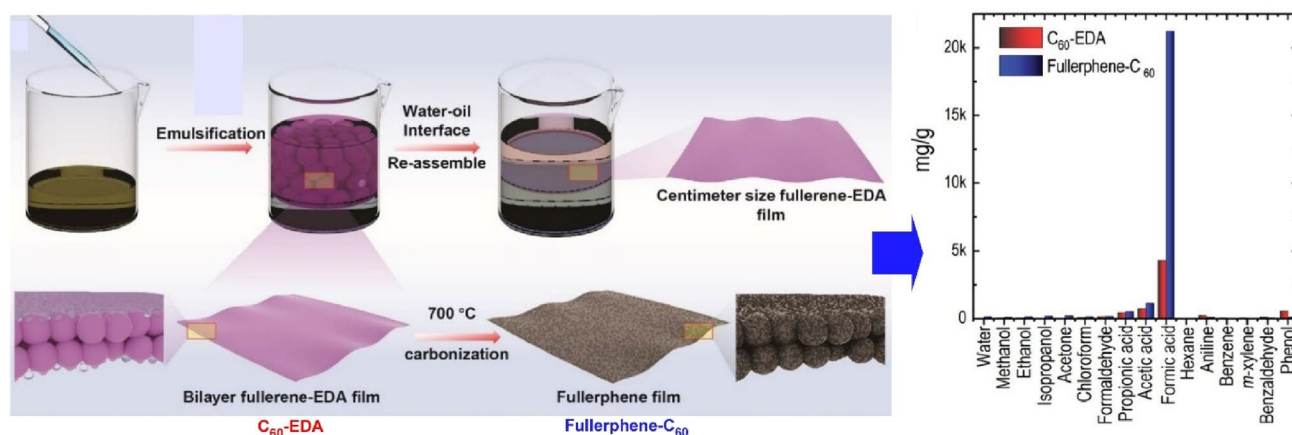


Fig. 17 Bottom-up fabrication of a novel, molecularly thin, nitrogen-doped 2D material called fullerphene: preparation (left); high selectivity between acetic acid and formic acid (right). The large surface

area and well-defined, ultrafine pores of fullerphene films are highly beneficial for vapour adsorption sensing processes. Reprinted with permission from Ref. 172. Copyright 2022 Wiley–VCH

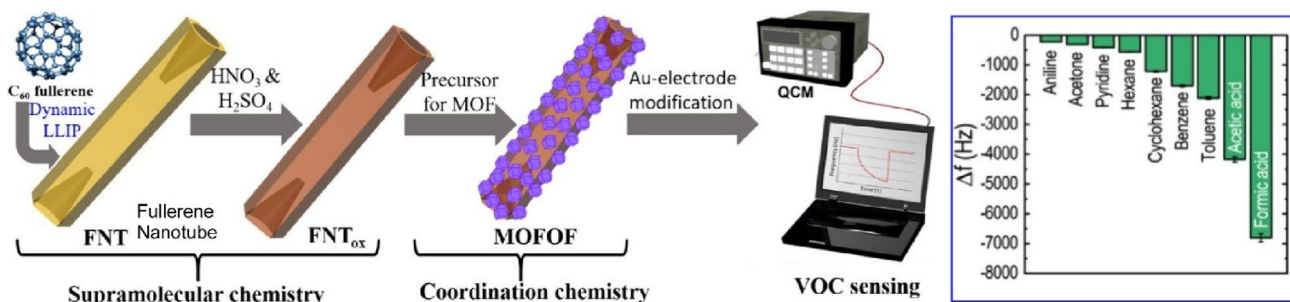
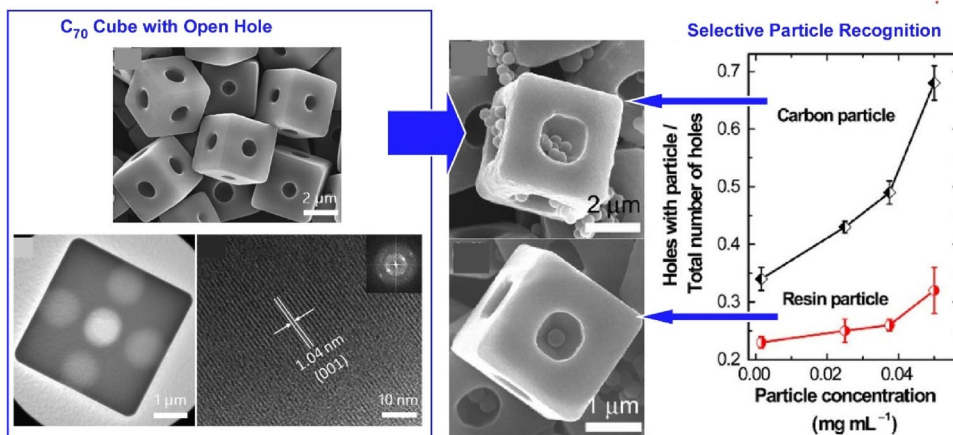


Fig. 18 A metal–organic framework on a fullerene aggregate (MOFOF): synthesis procedure involving the initial controlled fabrication of the fullerene as a tubular nanostructure (fullerene nanotube), followed by surface functionalisation and surface growth of the MOF (left); QCM sensor modified with MOFOF for a wide range of VOCs

were observed, with the sensitivity/selectivity order being formic acid > acetic acid > toluene > benzene > cyclohexane > hexane > pyridine > acetone > aniline (right). Reprinted with permission from Ref. 173 Copyright 2024 American Chemical Society

Fig. 19 Highly crystalline fullerene C_{70} cubes with open-hole structures in the centre of each face with preferential recognition capability for graphitic carbon particles over polymeric resin particles of similar dimensions. Due to the sp^2 -rich carbon material nature of the cubes, the open-hole cubes can preferentially recognise graphitic carbon particles over polymeric resin particles of similar dimensions. Reprinted with permission from Ref. 174 Copyright 2017 American Chemical Society



an electron beam. Due to the sp^2 -rich carbon material nature of the cubes, the open-hole cubes can preferentially recognise graphitic carbon particles over polymeric resin particles of similar dimensions. Specifically, the incorporation of resorcinol–formaldehyde polymeric resin particles and graphitic carbon particles into the open holes was observed. SEM observation revealed that most of the open holes on the cubes were occupied by graphitic carbon particles. This leads to selective sensing of particles. This could be useful for developing key materials for micro/nanoencapsulation processes. These processes have many applications, such as the controlled release of drugs, cosmetics and pigments, the protection of bioactive species and the removal of pollutants.

As a structure capable of identifying and sensing particles, Tang et al. fabricated a fullerene microhorn (Fig. 20) [175]. First, they prepared a fullerene microtube containing a solid core that bisected a tubular cavity, using a solution containing a mixture of C_{60} and C_{70} fullerenes. Exposure to an alcohol/mesitylene mixture at 25 °C caused the microtube to change structure, forming a microhorn. Due to the low solubility of C_{70} and C_{60} fullerenes in the solvent, the C_{60} and C_{70} cocrystal distribution is not uniform. The solid

core of the microtube contains a high concentration of C_{70} , whereas the tubular part mainly comprises small amounts of C_{60} and C_{70} . Consequently, when a mesitylene/*tert*-butyl alcohol solvent mixture is added to the microtube to induce a secondary transformation of its structure, the C_{70} -rich solid core dissolves in the solvent due to C_{70} 's higher solubility in mesitylene than C_{60} 's. This results in the microtube separating into two microhorns. The cone-shaped microhorn is hollow inside. The strong electrostatic interaction between the negatively charged microhorn and positively charged silica particles allows preferential recognition of silica particles over fullerene C_{70} , polystyrene latex, polystyrene hydroxylate or polystyrene carboxylate particles of a similar size. SEM observations revealed a greater number of silica particles on the surface and inside the fullerene microhorn than C_{70} particles at all concentrations. The hollow morphology of the microhorn may have greater application potential in various fields, such as sensing and microencapsulation of target particles.

This section has demonstrated the creation of a variety of structures using simple, elemental and structural fullerenes. Examples include: hierarchical structures with mesoporous nanorods extending from the surface of a cube;

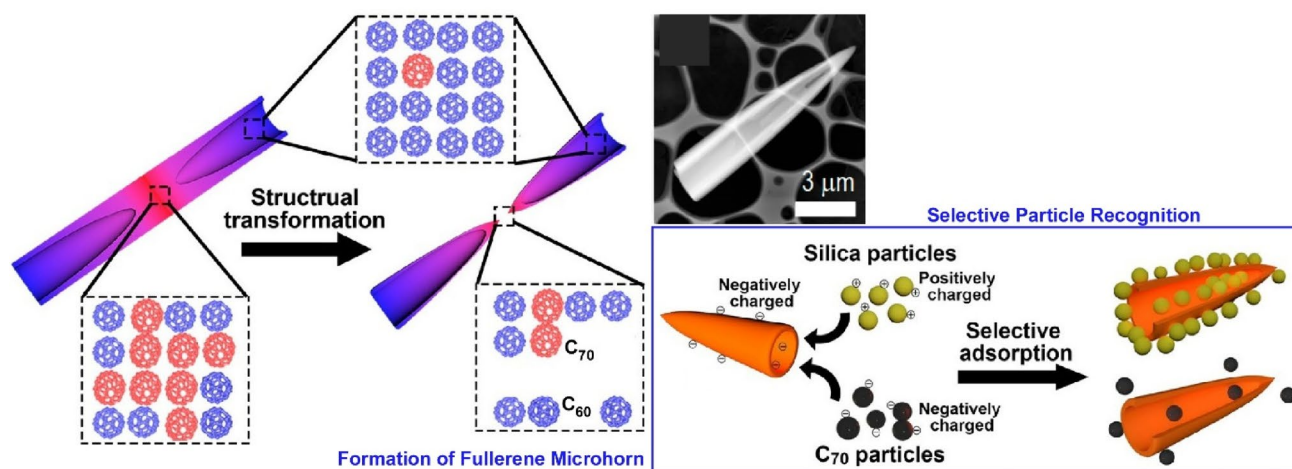


Fig. 20 Fabricated a fullerene microhorn through first formation of a fullerene microtube using a solution containing a mixture of C_{60} and C_{70} fullerenes and conversion to a microhorn upon exposure to an alcohol/mesitylene mixture (left), which exhibits preferential recog-

nition of silica particles over fullerene C_{70} , polystyrene latex, polystyrene hydroxylate or polystyrene carboxylate particles of a similar size (right). Reprinted with permission from Ref. 175 Copyright 2019 American Chemical Society

intricate structures created by face-selective chemical etching of crystals; fullerene rosettes; a two-dimensional material created by the simultaneous assembly and reaction of fullerenes; a two-dimensional, sheet-like structure called fullerphene; a new material called a MOF hybridized with fullerene. These structures offer high sensitivity to sensing due to their antenna structure, high surface area, nanoporous structure and composite structure. These structural characteristics also enable selective sensing based on aromaticity, hydrophobicity, acidity/basicity and size differences of one atom. Fabricating these structures also allows for greater control over their structure. The fabrication of highly crystalline fullerene cubes with open holes in the centre of each face, as well as fullerene microhorn structures, has been demonstrated. The properties of these nano/microstructured surfaces enable the construction of sensing systems that can recognise graphitic carbon or silica particles preferentially. These examples demonstrate that various structures can be constructed from simple units using nanoarchitecture. Furthermore, these structures exhibit diverse sensing properties. Nanoarchitectonics, which involves assembling structures from simple molecular units in a bottom-up manner, shows great potential for developing sensing materials.

4 Materials Nanoarchitectonics on Sensor Device Structures

The above section focused on sensing structures and materials. In particular, it showed how a variety of sensing structures can be constructed from simple unit molecules using

nanoarchitectonics. The next section will present examples of nanoarchitectonics incorporating sensing device structures.

A sensor receives an external object or stimulus and converts it into an electrical signal. If we could construct a material system whose conductivity changed in response to an external stimulus, it could easily be combined with various existing devices. For example, this goal would be met if the conductivity of an organic semiconductor could be adjusted by an external reaction. Ishii, Yamashita and their colleagues developed a method of controlling the Fermi level of a semiconductor using proton-coupled electron transfer, a process that is widely used in biochemistry (Fig. 21) [176]. Chemical doping was achieved by simply immersing a p-type organic semiconductor thin film in an aqueous solution containing a proton-coupled electron-transfer redox couple and hydrophobic molecular ions. A pair of quinone and benzoquinone was used as the redox couple. The synergistic reaction of proton-coupled electron transfer and the intercalation of hydrophobic ions enabled the efficient chemical doping of a crystalline organic semiconductor thin film at room temperature. According to the Nernst equation, the Fermi level of an organic semiconductor thin film is controlled by proton activity. Therefore, a resistive pH sensor that does not require a reference electrode is also possible, based on this method. This doping control mechanism can be coupled to any chemical or biochemical process that can alter proton activity. Therefore, this mechanism has potential applications in biosensors and bioelectronics. Since the process can be performed in aqueous solutions at room temperature and pressure, it is highly scalable in practice. It will serve as a platform for ambient semiconductor processing and biomolecular electronics. In addition, further systematic

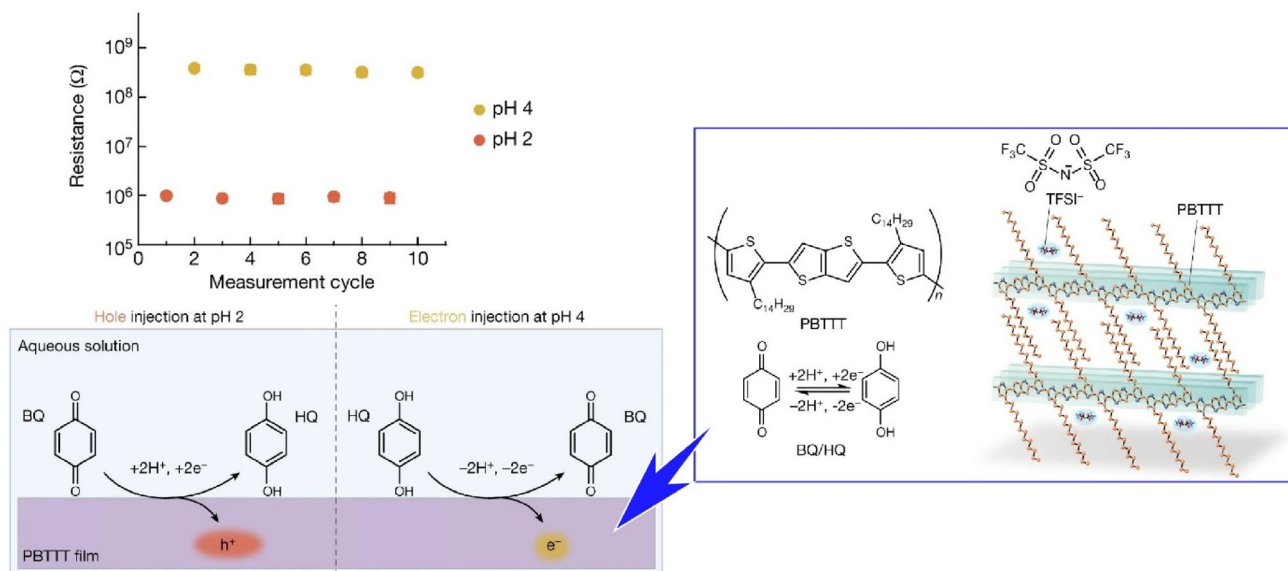


Fig. 21 A method of controlling the Fermi level of a polymer semiconductor film using proton-coupled electron transfer, enabling a resistive pH sensor that does not require a reference electrode. According to the Nernst equation, the Fermi level of an organic semiconductor thin

film is controlled by proton activity. Therefore, a resistive pH sensor that does not require a reference electrode is also possible, based on this method. Reprinted with permission from Ref. 176 Copyright 2023 Springer-Nature

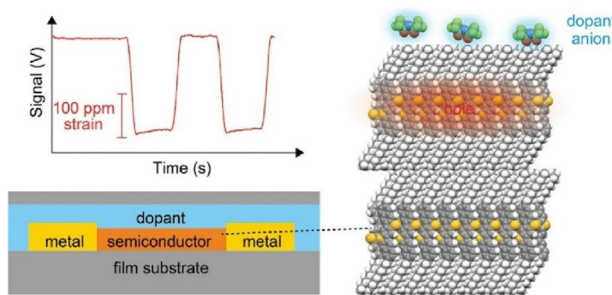


Fig. 22 A resistive strain sensor through the stable and effective p-type chemical doping of organic semiconductor single crystals. The shift in signal voltage upon repeated application of 230 ppm strain was monitored. Based on the time-averaged data, the gauge factor was calculated to be 22. Reproduced under terms of the CC-BY license from Ref. 177, 2025 Taylor & Francis

investigations through energy band diagrams would specify the other possible combinations for Fermi level regulation by proton-coupled electron transfer.

Organic semiconductor single crystals offer flexibility, can be processed using solutions, and enable high-mobility coherent carrier transport. These properties make them ideal for use in printed flexible electronics applications. Mechanical strain sensors can be fabricated using organic semiconductor single crystals as the active channel. Yamashita and colleagues fabricated resistive strain sensors through the stable and effective p-type chemical doping of organic semiconductor single crystals (Fig. 22) [177]. In this approach, 3,11-dinonyldinaphtho[2,3-d:2',3'-d']benzo[1,2-b:4,5-b']dithiophene was used as the organic semiconductor and its single-crystal film was prepared using a continuous

edge-casting method. Strain sensors based on this single crystal were fabricated using an ion-exchange doping method. This produced organic semiconductor crystalline thin films on 10 cm substrates, with a uniform and scalable fabrication and doping process. The sensor structure is designed to accurately measure resistance changes with a low noise level using a Wheatstone bridge circuit and a compact lock-in amplifier. Significant noise reduction was achieved, enabling highly accurate signal measurement with an accuracy of ± 1.8 ppm. The shift in signal voltage upon repeated application of 230 ppm strain was monitored. Based on the time-averaged data, the gauge factor was calculated to be 22. These results demonstrate the scalable fabrication of highly accurate and reliable organic semiconductor strain sensors, expanding their potential applications in various industrial fields.

A sensitive sensor can be created using hybrid nanoarchitectonics to incorporate a sensitive thin film into a new type of sensor system called a membrane-type surface stress sensor (MSS). An MSS consists of a silicon-based membrane that is suspended by four sensing beams, forming a Wheatstone bridge. Each sensing beam is embedded with a piezoresistor via boron doping. Maji et al. developed a sensing device to monitor volatile fatty acids — a key intermediate during bioreactor operation — in the headspace of an anaerobic reactor (Fig. 23) [178]. Anaerobic digesters have the potential to become a major source of green energy in a future sustainable society. To achieve this, the effective operating parameters of the reactor must be established and maintained through automation. Real-time estimation

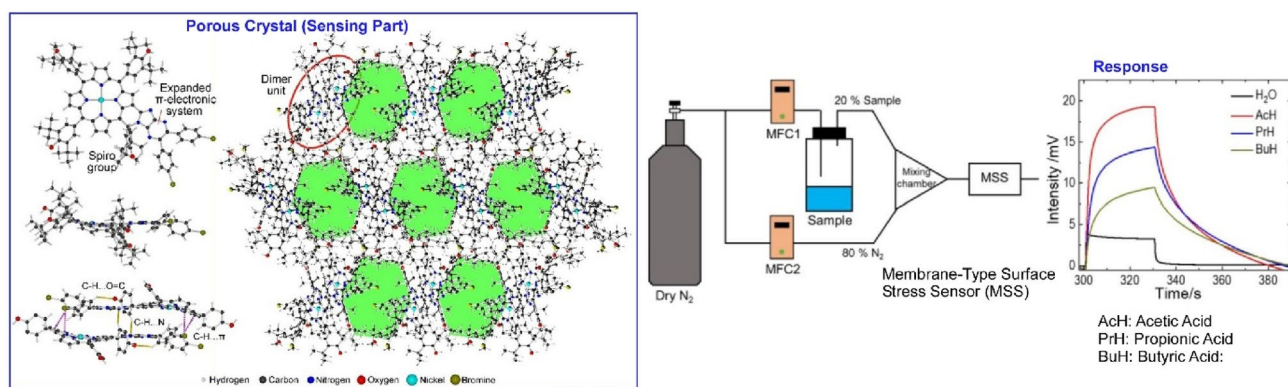
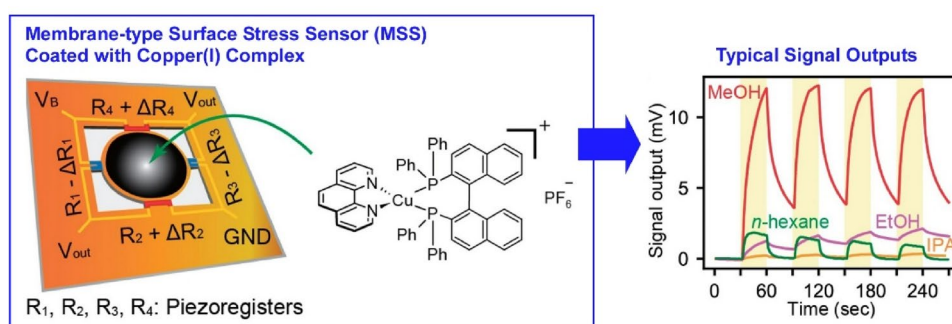


Fig. 23 A membrane-type surface stress sensor (MSS) with porous materials of porphyrin derivatives for real-time estimation of the volatile fatty acid content in the reactor headspace is therefore necessary. In this sensor, porphyrin derivatives were inkjet printed onto the MSS

membrane surface, and single crystals were grown within a microporous structure. Reprinted with permission from Ref. 178 Copyright 2025 Wiley–VCH

Fig. 24 A copper(I) complex-coated MSS system to be used as a platform for the specific sensing of methanol. Typical response profiles are shown in right-hand side. Reprinted with permission from Ref. 179 Copyright 2021 Oxford University Press



of the volatile fatty acid content in the reactor headspace is therefore necessary. Porphyrin derivatives were inkjet printed onto the MSS membrane surface, and single crystals were grown within a microporous structure. The sensor system demonstrated excellent sensitivity to each acid vapour, with the highest sensitivity to acetic acid. In particular, its extremely low sensitivity and selectivity to water vapour make it ideal for real-time sensing applications. This sensor principle can also be used for other purposes. The presence and composition of volatile fatty acids in the human gut microbiome are important factors in determining general digestive health. They have also been reported to affect several pathologies, including cancer and cognitive function. It is expected that the in situ system for volatile fatty acids will be widely applied to these important targets.

Nishikawa et al. successfully fabricated a copper(I) complex-coated MSS system to be used as a platform for the specific sensing of methanol molecules (Fig. 24) [179]. The sensing performance of various volatile organic compounds was investigated based on the transmission of mechanical stress derived from the sorption-induced deformation of the Cu(I) complex. The fabricated sensor device exhibited a selective response to methanol in the presence of a wide range of volatile organic compounds. The complex metal centre is surrounded by hydrogen atoms of aromatic C-H

bonds or fluorine atoms of the PF_6^- anion, and it is this weak interaction between these moieties that favours the effective absorption of methanol. The rigid, sterically hindered ligand effectively forms a dense receptor layer with limited intermolecular space, enabling sensitive discrimination of small molecules. A clear MSS signal response was also observed upon exposure to methanol samples that were trace-mixed in n-hexane and gasoline. The response to the methanol blend was higher than that to the ethanol blend. In fact, gasoline vapour containing 1% methanol produced a much higher MSS response than the gasoline sample containing 20% ethanol. Contamination of gasoline and related petroleum samples with methanol is a common problem in the automotive and fuel sectors worldwide. The results of this study will help to address this societal issue.

The ability to detect trace amounts of water in organic solvents is of great importance in chemistry and industry. Although Karl Fischer titration has traditionally been used for this purpose, it has some limitations in terms of rapid and direct detection due to the time-consuming nature of sample preparation and the specific instrument requirements involved. As an alternative, Murata et al. developed an MSS nanomechanical sensor with DNA immobilised using an inkjet printer (Fig. 25) [180]. To estimate the selectivity of the DNA-coated MSS sensor for water, the response to six

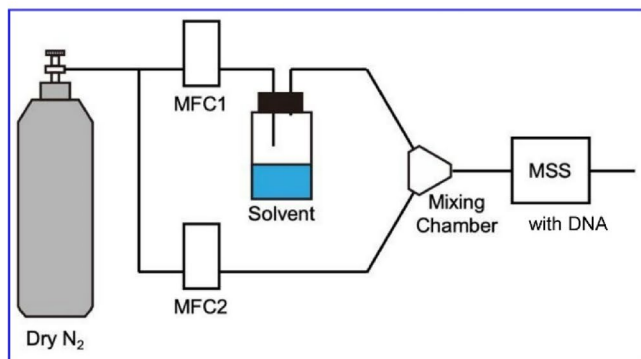
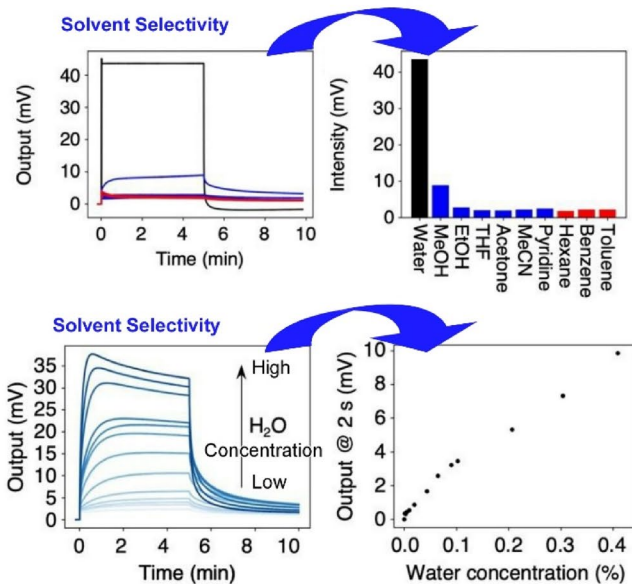


Fig. 25 A MSS nanomechanical sensor with DNA immobilised using an inkjet printer capable of detection of trace amounts of water at the limit of detection of ppb. The response to six water-miscible organic solvents (methanol, ethanol, tetrahydrofuran, acetone, acetonitrile and

water-miscible organic solvents (methanol, ethanol, tetrahydrofuran, acetone, acetonitrile and pyridine), three water-immiscible solvents (n-hexane, benzene and toluene) and ten vapours containing water was measured. High sensitivity and selectivity to water vapour were demonstrated. Additionally, trace amounts of water in organic solvents could be detected. Trace amounts of water could be successfully detected and quantified in the vapour at the limit of detection of ppb. Compared with Karl Fischer titration, water content could be quantified in a shorter amount of time. Furthermore, when determining the water content in tetrahydrofuran, a signal was produced two seconds after vapour injection. The chemical reactions used in Karl Fischer titration usually require a base reagent, such as pyridine, so Karl Fischer titration is not applicable to all solvents. Therefore, the DNA-based nanomechanical sensor could be used as an alternative to Karl Fischer titration. It provides a simple, rapid method for detecting and quantifying trace amounts of water in various organic solvents.

Using the inkjet method, it is difficult to create a thin film with molecular-level smoothness, and there may be variation in the quality of each sample. To address this issue, Murata et al. developed a method of fabricating a solid, nanometre-flat DNA thin film using a DNA source extracted from salmon sperm and laser molecular beam deposition under high vacuum conditions (Fig. 26) [181]. While the cast film was uneven by about 100 nm, the film produced using the laser molecular beam deposition method was uneven by no more than the measurement noise range (with an average



pyridine), three water-immiscible solvents (n-hexane, benzene and toluene) and ten vapours containing water was measured. High sensitivity and selectivity to water vapour were demonstrated. Reproduced under terms of the CC-BY license from Ref. 180, 2022 MDPI

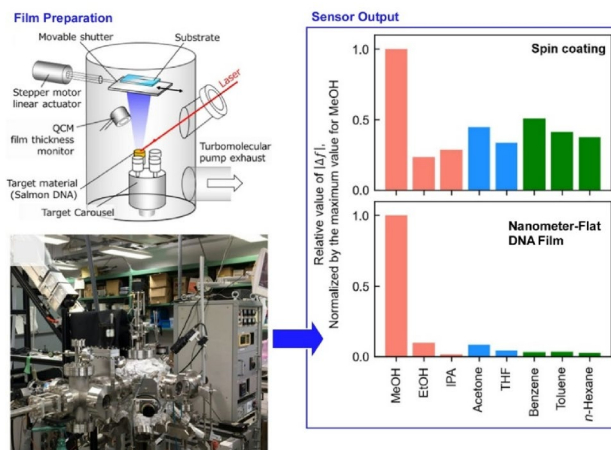


Fig. 26 Fabrication of nanometre-flat DNA thin film using laser molecular beam deposition under high vacuum conditions for a QCM sensor with greater methanol detection ability. A QCM sensor fabricated with a DNA thin film using laser molecular beam deposition exhibited greater methanol detection ability than a sensor using a DNA thin film fabricated by spin coating. Reprinted with permission from Ref. 181 Copyright 2022 Oxford University Press

surface roughness of 7.4 nm). Spectrum analysis revealed fragmentation due to cleavage of phosphate bonds, yet the DNA thin film formed by the laser molecular beam deposition method exhibited molecular flatness. Volatile organic compounds such as methanol, ethanol, 2-propanol, acetone, tetrahydrofuran, toluene, benzene and n-hexane were examined. A QCM sensor fabricated with a DNA thin film using laser molecular beam deposition exhibited greater methanol detection ability than a sensor using a DNA thin film

fabricated by spin coating. The reproducibility of the sensor response to methanol was confirmed by repeatedly switching between methanol vapour and nitrogen gas. This deposition method can produce uniform films over large areas and is therefore suitable for mass production. It is expected that this method will be applied to a wide range of potential biomolecular sensing thin films.

This section has presented examples of sensor structures constructed as a hybrid of sensing films and device structures. A method of controlling the Fermi level of semiconductors has been developed using proton-coupled electron-transfer, a process that is widely used in biochemical reactions. According to the Nernst equation, the Fermi level of organic semiconductor thin films is influenced by proton activity. This could lead to the development of resistive pH sensors that do not require a reference electrode. Organic semiconductor single crystals offer flexibility, solution processability and high-mobility coherent carrier transport. These properties enable the fabrication of mechanical strain sensors using organic semiconductor single crystals as the active channel. Sensitive sensors can also be fabricated using hybrid nanoarchitectonics to incorporate sensitive thin films into a new type of sensor system called MSS. Porphyrin derivatives can be inkjet-printed onto MSS membrane surfaces to grow single crystals with a microporous structure, resulting in sensors that show excellent sensitivity to acid vapour. Notably, they exhibit the lowest sensitivity and selectivity to water vapour, offering significant advantages for real-time sensing applications. Furthermore, it has been demonstrated that MSS systems coated with copper(I) complexes can be used as a novel sensing platform for specific molecular detection. The weak interaction between these moieties enables effective methanol absorption, allowing trace amounts of methanol to be detected in gasoline. MSS nanomechanical sensors with inkjet-immobilised DNA showed high sensitivity and selectivity to water vapour, enabling the detection of trace amounts of water in organic solvents. They have succeeded in detecting and quantifying water at parts per billion (ppb) levels in solvents through the vapour. There have also been innovations in thin film fabrication methods. A DNA source extracted from salmon sperm was used in a laser molecular beam deposition method under high vacuum conditions to develop a technique for producing solid thin films featuring nanometre-flat DNA. A sensor fabricated with this film on a QCM electrode exhibited greater methanol detection capabilities than a sensor using a spin-coated DNA thin film.

Nanoarchitectonics encompasses a range of material chemistry approaches, including molecular assembly and thin film fabrication, as well as fabrication methods for creating devices. It is a methodology suitable for fabricating material and device structures. Coupling molecular

reactions, molecular recognition and external stimuli with the doping behaviour and conductivity of organic semiconductors enables the creation of sensing systems that integrate stimuli and signals. Additionally, the hybrid nanoarchitectonics of sensitive films and new devices can produce highly sensitive sensors for various targets. Developing functional structures by combining multiple processes based on the concept of nanoarchitectonics is beneficial for sensor development.

5 Future Perspectives

This review article has adopted a methodology of examining examples of sensors and sensing functions, limited to recent papers with the word ‘nanoarchitectonics’ in the title. The materials and applications used are generally very diverse. A notable trend is the development of sensors for increasingly complex targets, such as biomaterials and biological phenomena. Creating such recognition structures necessitates sophisticated construction techniques. Nanoarchitectonics should play a significant role in integrating technologies to create functional structures. To demonstrate that various structures can be prepared using nanoarchitectonics from simple units, this review article presents an approach to constructing sensing structures from the bottom up nanoarchitectonics based on fullerenes. Using the nanoarchitectonics approach, hierarchical sensing structures that can accommodate various recognition sizes can be developed from simple units of a single element in zero dimensions. Nanoarchitectonics broadly encompasses material chemistry approaches and fabrication methods for device creation, making it a suitable methodology for fabricating material/device structures. Coupling molecular reactions, molecular recognition and external stimuli with the doping behaviour and electrical conductivity of organic semiconductors makes it possible to create sensing systems that integrate stimuli and signals. Furthermore, hybrid nanoarchitectonics of sensitive films and devices can be employed to produce highly sensitive sensors for various targets. Nanoarchitectonics provides a methodology for developing functional structures by combining multiple processes, which is beneficial for sensor development.

The nanoarchitectonics approach involves building up molecules, materials or device structures and is ideal for creating selective recognition structures for molecules, materials, or stimuli. It is also useful for creating organizations that efficiently transmit signals. The concept of nanoarchitectonics is therefore used in many sensor research projects. Finally, I would like to consider some avenues for future research. As demonstrated by numerous sensor examples, there is a high demand for bio-based sensors. Demand for

sensors that can detect viruses, monitor lifestyle-related diseases and enable the early detection of serious diseases will continue to grow. Consequently, the need for sensor development using nanoarchitectonics that takes biocompatibility into consideration will also increase. Biosystems are made by assembling molecules and materials in a rational way, and they have many things in common with nanoarchitectonics. Bio-oriented nanoarchitectonics is a widely considered approach [182, 183]. More advanced systems involve developing small, remote-controlled sensor devices that can move autonomously within the body. There is also discussion about building nano/micro robots using nanoarchitectonics [184, 185]. Additionally, sensor systems for detecting various signals and stimuli must be developed, as well as methods for analysing complex responses resulting from multiple inputs using artificial intelligence. Based on this information, combining nanoarchitectonics with machine learning and material informatics will be necessary to build more capable sensor systems. The importance of collaboration between nanoarchitectonics and materials informatics has also been highlighted in other material systems [186]. For practical applications, developing fabrication methods suitable for mass production and creating reliable devices will be essential. Methods such as edge casting for organic semiconductors and laser molecular beam deposition for biomolecules have been devised. Utilization of nanoarchitectonics approaches in hybrid, composite, and other related materials has been widely researched for many functions [187–191]. The most important challenges in sensor nanoarchitectonics would be establishments of standard methodology to create commercially available sensors with nanoarchitectonics concepts. Some gaps still remain between basic science and market demand. Some bottlenecks including mass production cost and long-term stability have to be solved. In the nanoarchitectonics approach to sensor development for practical uses, developing basic fabrication technology to create thin film structures of reliable quality over a large area would be crucially important. It should be suggested to propose more specific research goals based on current technical bottlenecks, mass production cost and long-term stability, such as developing scalable laser molecular beam deposition processes to reduce the cost of biosensing thin films.

This paper examines examples of sensor development using nanoarchitectonics and related approaches, exploring their trends and characteristics. The extremely wide range of applications suggests a variety of possibilities. Further development will require the creation of systems better suited to biotechnology, the integration of nano/micro robots, the utilisation of artificial intelligence and the improvement of fabrication technology for mass production and industrialisation.

Acknowledgements This study was partially supported by Japan Society for the Promotion of Science KAKENHI (Grant Numbers, JP23H05459 and JP25H00898).

Author Contributions This is a single author paper. This author takes all the tasks.

Funding Funding was provided by Japan Society for the Promotion of Science, JP25H00898

Data Availability No datasets were generated or analysed during the current study.

Declarations

Conflict of interest The authors declare no competing interests.

Open Access This article is licensed under a Creative Commons Attribution 4.0 International License, which permits use, sharing, adaptation, distribution and reproduction in any medium or format, as long as you give appropriate credit to the original author(s) and the source, provide a link to the Creative Commons licence, and indicate if changes were made. The images or other third party material in this article are included in the article's Creative Commons licence, unless indicated otherwise in a credit line to the material. If material is not included in the article's Creative Commons licence and your intended use is not permitted by statutory regulation or exceeds the permitted use, you will need to obtain permission directly from the copyright holder. To view a copy of this licence, visit <http://creativecommons.org/licenses/by/4.0/>.

References

1. D. Guo, R. Shibuya, C. Akiba, S. Saji, T. Kondo, J. Nakamura, Active sites of nitrogen-doped carbon materials for oxygen reduction reaction clarified using model catalysts. *Science* **351**(6271), 361–365 (2016). <https://doi.org/10.1126/science.aad0832>
2. P. Ganesan, A. Ishihara, A. Staykov, N. Nakashima, Recent advances in nanocarbon-based nonprecious metal catalysts for oxygen/hydrogen reduction/evolution reactions and Zn-air battery. *Bull. Chem. Soc. Jpn* **96**(5), 429–443 (2023). <https://doi.org/10.1246/bcsj.20230051>
3. T. Fukushima, M. Higashi, M. Yamauchi, Carbon-neutral energy cycle via highly selective electrochemical reactions using biomass derivable organic liquid energy carriers. *Bull. Chem. Soc. Jpn* **96**(11), 1209–1215 (2023). <https://doi.org/10.1246/bcsj.20230172>
4. T. Nakamura, Y. Kondo, N. Ohashi, C. Sakamoto, A. Hasegawa, S. Hu, M.A. Truong, R. Murdey, Y. Kanemitsu, A. Wakamiya, *Bull. Chem. Soc. Jpn* **97**, uoad025 (2024)
5. K. Hayashida, J. Nakamura, K. Takeyasu, Why does the performance of nitrogen-doped carbon electrocatalysts decrease in acidic conditions? *Angew. Chem. Int. Ed.* **64**(26), e202502702 (2025). <https://doi.org/10.1002/anie.202502702>
6. A. Fukuoka, *Bull. Chem. Soc. Jpn* **96**, 1071 (2023)
7. J. Wang, F. Matsuzawa, N. Sato, Y. Amano, M. Machida, Preparation of nitrogen-doped glucose-derived activated carbon and its application for the efficient removal of phosphate ions from aqueous solution. *Bull. Chem. Soc. Jpn* **96**(10), 1088–1098 (2023). <https://doi.org/10.1246/bcsj.20230106>
8. K. Kadota, S. Horike, *Acc. Chem. Res.* **57**, 3206 (2024)

9. S. Liang, H. Feng, N. Chen, B. Wang, M. Hu, X.X. Huang, K. Yang, Y. Gu, *Bull. Chem. Soc. Jpn* **97**, uoae054 (2024)
10. M.S. Hossain, Y. Hoshino, H. Shimakoshi, High-performance and recyclable multisite catalytic system for CO₂ fixation using crown ether-linked Schiff base and alkali halides. *Adv. Synth. Catal.* **367**(11), e202500246 (2025). <https://doi.org/10.1002/adsc.202500246>
11. Y. Miyahara, N. Nagaya, M. Kataoka, B. Yanagawa, K. Tanaka, H. Hao, K. Ishino, H. Ishida, T. Shimizu, K. Kangawa, S. Sano, T. Okano, S. Kitamura, H. Mori, Monolayered mesenchymal stem cells repair scarred myocardium after myocardial infarction. *Nat. Med.* **12**(4), 459–465 (2006). <https://doi.org/10.1038/nm1391>
12. T. Niwa, T. Tahara, C.E. Chase, F.G. Fang, T. Nakaoka, S. Irie, E. Hayashinaka, Y. Wada, H. Mukai, K. Masutomi, Y. Watanabe, Y. Cui, T. Hosoya, Synthesis of ¹¹C-radiolabeled eribulin as a companion diagnostics PET tracer for brain glioblastoma. *Bull. Chem. Soc. Jpn* **96**(3), 283–290 (2023). <https://doi.org/10.1246/bcsj.20220335>
13. T. Miura, T.R. Malla, L. Brewitz, A. Tumber, E. Salah, K.J. Lee, N. Terasaka, C.D. Owen, C. Strain-Damerell, P. Lukacik, M.A. Walsh, A. Kawamura, C.J. Schofield, T. Katoh, H. Suga, *Bull. Chem. Soc. Jpn* **97**, uoae018 (2024)
14. A. Alowasheer, M. Eguchi, Y. Fujita, K. Tsuchiya, R. Wakabayashi, T. Kimura, K. Ariga, K. Hatano, N. Fukumitsu, Y. Yamauchi, *Bull. Chem. Soc. Jpn* **97**, uoae099 (2024)
15. M. Takeda, S. Yoshida, T. Inoue, Y. Sekido, T. Hata, A. Hamabe, T. Ogino, N. Miyoshi, M. Uemura, H. Yamamoto, Y. Doki, H. Eguchi, The role of KRAS mutations in colorectal cancer: biological insights, clinical implications, and future therapeutic perspectives. *Cancers* **17**(3), 428 (2025). <https://doi.org/10.3390/cancers17030428>
16. K.N. Ferreira, T.M. Iverson, K. Maghlaoui, J. Barber, S. Iwata, *Science* **303**, 1831 (2004)
17. Y. Umena, K. Kawakami, J.-R. Shen, N. Kamiya, *Nature* **473**, 55 (2011)
18. K. Kato, M. Kumazawa, Y. Nakajima, T. Suzuki, N. Dohmae, J.R. Shen, K. Ifuku, R. Nagao, *Sci. Adv.* **11**, eadv7488 (2025)
19. H. Imahori, Molecular photoinduced charge separation: fundamentals and application. *Bull. Chem. Soc. Jpn* **96**(4), 339–352 (2023). <https://doi.org/10.1246/bcsj.20230031>
20. S. Watanabe, K. Oyaizu, Designing strategy for high refractive index polymers: from the molecular level to bulk structure control. *Bull. Chem. Soc. Jpn* **96**(10), 1108–1128 (2023). <https://doi.org/10.1246/bcsj.20230177>
21. S.-Q. Wu, S.-Q. Su, S. Kanegawa, O. Sato, *Acc. Chem. Res.* **58**, 1284 (2025)
22. J. Tanks, T. Hiroi, K. Tamura, K. Naito, Tethering organic disulfides to layered silicates: a versatile strategy for photo-controllable dynamic chemistry and functionalization. *Bull. Chem. Soc. Jpn* **96**(1), 65–71 (2023). <https://doi.org/10.1246/bcsj.20220309>
23. S. Horike, Glass and liquid chemistry of coordination polymers and MOFs. *Bull. Chem. Soc. Jpn* **96**(9), 887–898 (2023). <https://doi.org/10.1246/bcsj.20230152>
24. K. Nishikawa, K. Fujii, K. Matsumoto, H. Abe, M. Yoshizawa-Fujita, *Bull. Chem. Soc. Jpn* **97**, uoae088 (2024)
25. A.P. Millán, H. Sun, L. Giambagli, R. Muolo, T. Carletti, J.J. Torres, F. Radicchi, J. Kurths, G. Bianconi, *Nat. Phys.* **21**, 353 (2025)
26. T. Yamada, Y. Hayamizu, Y. Yamamoto, Y. Yomogida, A. Izadi-Najafabadi, D.N. Futaba, K. Hata, A stretchable carbon nanotube strain sensor for human-motion detection. *Nat. Nanotechnol.* **6**(5), 296–301 (2011). <https://doi.org/10.1038/nnano.2011.36>
27. P.H. Syaifee, M.A.F. Nasution, I. Rahmawati, E. Saepudin, T.A. Ivandini, *Bull. Chem. Soc. Jpn* **97**, uoad007 (2024)
28. K. Sato, M. Gon, K. Tanaka, Y. Chujo, *Bull. Chem. Soc. Jpn* **97**, uoae040 (2024)
29. J.S.S.K. Formen, J.R. Howard, E.V. Anslyn, C. Wolf, Circular dichroism sensing: strategies and applications. *Angew. Chem. Int. Ed.* **63**(19), e202400767 (2024). <https://doi.org/10.1002/anie.202400767>
30. T. Kaneda, K. Kato, S. Ohtani, T. Ogoshi, *Bull. Chem. Soc. Jpn* **97**, uoae093 (2024)
31. M. Sugiyama, M. Akiyama, Y. Yonezawa, K. Komaguchi, M. Higashi, K. Nozaki, T. Okazoe, Electron in a cube: synthesis and characterization of perfluorocubane as an electron acceptor. *Science* **377**(6607), 756–759 (2022). <https://doi.org/10.1126/science.abq0516>
32. N. Tsubaki, Y. Wang, G. Yang, Y. He, Rational design of novel reaction pathways and tailor-made catalysts for value-added chemicals synthesis from CO₂ hydrogenation. *Bull. Chem. Soc. Jpn* **96**(3), 291–302 (2023). <https://doi.org/10.1246/bcsj.20220344>
33. Y. Inokuma, *Bull. Chem. Soc. Jpn* **97**, uoae072 (2024)
34. T. Yasukawa, *Bull. Chem. Soc. Jpn* **97**, uoae076 (2024)
35. N. Kai, H. Kono, T. Stünke, D. Imoto, R. Zanasi, G. Monaco, F.F. Summa, L.T. Scott, A. Yagi, K. Itami, *Chem. Sci.* **16**, 9195 (2025)
36. Y. Ohki, Biomimetic transition metal cluster complexes: synthetic studies and applications in the reduction of inert small molecules. *Bull. Chem. Soc. Jpn* **96**(7), 639–648 (2023). <https://doi.org/10.1246/bcsj.20230108>
37. H. Inaba, Y. Hori, A.M.R. Kabir, A. Kakugo, K. Sada, K. Matsuura, Construction of silver nanoparticles inside microtubules using Tau-derived peptide ligated with silver-binding peptide. *Bull. Chem. Soc. Jpn* **96**(10), 1082–1087 (2023). <https://doi.org/10.1246/bcsj.20230162>
38. T. Kosaka, Y. Niihori, T. Kawawaki, Y. Negishi, Synthesis of Au₁₃-based building block clusters for programmed dimer formation and Au₁₃ cluster dimer photoexcitation properties. *Nanoscale* **17**(20), 12695–12703 (2025). <https://doi.org/10.1039/D5NR00724K>
39. K. Kusada, H. Kitagawa, Phase control in monometallic and alloy nanomaterials. *Chem. Rev.* **125**(2), 599–659 (2025). <https://doi.org/10.1021/acs.chemrev.4c00368>
40. E. Yashima, N. Ousaka, D. Taura, K. Shimomura, T. Ikai, K. Maeda, Supramolecular helical systems: helical assemblies of small molecules, foldamers, and polymers with chiral amplification and their functions. *Chem. Rev.* **116**(22), 13752–13990 (2016). <https://doi.org/10.1021/acs.chemrev.6b00354>
41. M. Kamigaito, *Bull. Chem. Soc. Jpn* **97**, uoae069 (2024)
42. T. Yamamoto, A. Takahashi, H. Otsuka, *Bull. Chem. Soc. Jpn* **97**, uoad004 (2024)
43. Y. Kim, K. Iimura, N. Tamaoki, *Bull. Chem. Soc. Jpn* **97**, uoae034 (2024)
44. N. Kamiya, T. Kuroda, Y. Nagata, T. Yamamoto, M. Suginome, *J. Am. Chem. Soc.* **147**, 8534 (2025)
45. S. Kitagawa, R. Kitaura, S. Noro, *Angew. Chem. Int. Ed.* **43**, 2334 (2004)
46. B. Ay, R. Takano, T. Ishida, Metal-organodiphosphonate chemistry: hydrothermal syntheses and structures of two novel copper(II) coordination polymers with *o*-xylylenediphosphonic acid and 4,4'-bipyridine ligands. *Bull. Chem. Soc. Jpn* **96**(10), 1129–1138 (2023). <https://doi.org/10.1246/bcsj.20230160>
47. M. Nakai, K. Asano, K. Shimada, K. Kanno, Y. Nakabayashi, L. Alba, Y. Funahashi, S. Yano, H. Ishida, *Bull. Chem. Soc. Jpn* **97**, uoad017 (2024)
48. W. He, Y. Yu, K. Iizuka, H. Takezawa, M. Fujita, *Nat. Chem.* **17**, 653 (2025)
49. Y. Zhao, Y. Yamauchi, *Nat. Chem.* **17**, 161 (2025)
50. S. Datta, Y. Kato, S. Higashiharaguchi, K. Aratsu, A. Isobe, T. Saito, D.D. Prabhu, Y. Kitamoto, M.J. Hollamby, A.J. Smith, R. Dalgliesh, N. Mahmoudi, L. Pesce, C. Perego, G.M. Pavan, S. Yagai, *Nature* **583**, 400 (2020)

51. O. Oki, H. Yamagishi, Y. Morisaki, R. Inoue, K. Ogawa, N. Miki, Y. Norikane, H. Sato, Y. Yamamoto, *Science* **377**, 673 (2022)
52. H. Fujimoto, T. Hirao, T. Haino, *Bull. Chem. Soc. Jpn* **97**, uoad016 (2024)
53. N. Hara, H. Tamiaki, *Bull. Chem. Soc. Jpn* **97**, uoae032 (2024)
54. S. Datta, H. Itabashi, T. Saito, S. Yagai, *Nat. Chem.* **17**, 477 (2025)
55. J. Song, C. Yuan, T. Jiao, R. Xing, M. Yang, D.J. Adams, X. Yan, *Small* **16**, 1907309 (2020)
56. S. Nishimura, M. Tanaka, *Bull. Chem. Soc. Jpn* **96**, 1052 (2023)
57. B. Roy, T. Govindaraju, *Bull. Chem. Soc. Jpn* **97**, bcsj.20230224 (2024)
58. T. Hayashi, G.V. Latag, Self-assembled monolayers as platforms for nanobiotechnology and biointerface research: fabrication, analysis, mechanisms, and design. *ACS Appl. Nano Mater.* **8**(17), 8570–8587 (2025). <https://doi.org/10.1021/acsnm.5c00790>
59. D. Karna, S. Watanabe, G. Sharma, A. Sharma, Y. Zheng, I. Kawamata, Y. Suzuki, H. Mao, Logic-gated modulation of cell migration via mesoscale mechanical uncaging effects. *ACS Nano* **19**(8), 8058–8069 (2025). <https://doi.org/10.1021/acsnano.4c16194>
60. T. Adschiri, S. Takami, M. Umetsu, S. Ohara, T. Naka, K. Minami, D. Hojo, T. Togashi, T. Arita, M. Taguchi, M. Itoh, N. Aoki, G. Seong, T. Tomai, A. Yoko, Supercritical hydrothermal reactions for material synthesis. *Bull. Chem. Soc. Jpn* **96**(2), 133–147 (2023). <https://doi.org/10.1246/bcsj.20220295>
61. K. Ariga, S. Akakabe, R. Sekiguchi, M.L. Thomas, Y. Takeoka, M. Rikukawa, M. Yoshizawa-Fujita, *ACS Omega* **9**, 22203 (2024)
62. A. Kuzume, K. Yamamoto, *Bull. Chem. Soc. Jpn* **97**, uoae022 (2024)
63. V. Dananjaya, N. Hansika, S. Marimuthu, V. Chevali, Y.K. Mishra, A.N. Grace, N. Salim, C. Abeykoon, MXenes and its composite structures: synthesis, properties, applications, 3D/4D printing, and artificial intelligence; machine learning integration. *Prog. Mater. Sci.* **152**, 101433 (2025). <https://doi.org/10.1016/j.pmatsci.2025.101433>
64. H. Zhang, Y. Wang, Y. Zhu, P. Huang, Q. Gao, X. Li, Z. Chen, Y. Liu, J. Jiang, Y. Gao, J. Huang, Z. Qin, Machine learning and genetic algorithm-guided directed evolution for the development of antimicrobial peptides. *J. Adv. Res.* **68**, 415–428 (2025). <https://doi.org/10.1016/j.jare.2024.02.016>
65. T. Uematsu, N. Krobkrong, K. Asai, G. Motomura, Y. Fujisaki, T. Torimoto, S. Kuwabata, Bright red luminescence from Ag–In–Ga–S-based quantum dots with the introduction of copper. *Bull. Chem. Soc. Jpn* **96**(11), 1274–1282 (2023). <https://doi.org/10.1246/bcsj.20230216>
66. K. Saitow, *Bull. Chem. Soc. Jpn* **97**, uoad002 (2024)
67. S. Dasgupta, G. Cassone, F. Paesani, *J. Phys. Chem. Lett.* **16**, 2996 (2025)
68. Y. Liu, S. Shen, O.V. Prezhdo, R. Long, W.-H. Fang, *J. Am. Chem. Soc.* **147**, 11543 (2025)
69. Sd. Kalyana Sundaram, M.M. Hossain, M. Rezki, K. Ariga, S. Tsujimura, *Biosensors* **13**, 1018 (2023)
70. W. Yoshimune, *Bull. Chem. Soc. Jpn* **97**, uoae046 (2024)
71. G. Chen, M. Isegawa, T. Koide, Y. Yoshida, K. Harano, K. Hayashida, S. Fujita, K. Takeyasu, K. Ariga, J. Nakamura, Pentagon-rich caged carbon catalyst for the oxygen reduction reaction in acidic electrolytes. *Angew. Chem. Int. Ed.* **63**(49), e202410747 (2024). <https://doi.org/10.1002/anie.202410747>
72. Y. Sugimoto, P. Pou, M. Abe, P. Jelinek, R. Pérez, S. Morita, Ó. Custance, *Nature* **446**, 64 (2007)
73. M. Koshino, T. Tanaka, N. Solin, K. Suenaga, H. Isobe, E. Nakamura, *Science* **316**, 853 (2007)
74. K. Tada, Y. Hinuma, S. Ichikawa, S. Tanaka, Investigation of the interaction between Au and brookite TiO₂ using transmission electron microscopy and density functional theory. *Bull. Chem. Soc. Jpn* **96**(4), 373–380 (2023). <https://doi.org/10.1246/bcsj.20230007>
75. T. Nakamuro, *Bull. Chem. Soc. Jpn* **97**, uoae082 (2024)
76. Y. Okawa, M. Aono, *Nature* **409**, 683 (2001)
77. R. Waser, M. Aono, Nanoionics-based resistive switching memories. *Nat. Mater.* **6**(11), 833–840 (2007). <https://doi.org/10.1038/nmat2023>
78. S. Kawai, O. Krejčí, T. Nishiuchi, K. Sahara, T. Kodama, R. Pawlak, E. Meyer, T. Kubo, A.S. Foster, *Sci. Adv.* **6**, eaay8913 (2020)
79. Y. Hashikawa, Y. Murata, *Bull. Chem. Soc. Jpn* **96**, 943 (2023)
80. K. Kimura, K. Miwa, H. Imada, M. Imai-Imada, S. Kawahara, J. Takeya, M. Kawai, M. Galperin, Y. Kim, *Nature* **570**, 210 (2019)
81. N. Oyamada, H. Minamimoto, T. Fukushima, R. Zhou, K. Mura-koshi, *Bull. Chem. Soc. Jpn* **97**, uoae007 (2024)
82. T. Tahara, *Bull. Chem. Soc. Jpn* **97**, uoae012 (2024)
83. E. Mieda, Y. Morishima, T. Watanabe, H. Miyake, S. Shinoda, *Bull. Chem. Soc. Jpn* **96**, 538 (2023)
84. K. Saito, Y. Yamamura, Reticular-chemical approach to soft-matter self-assembly: why are *srs* and *noh* nets realized in thermotropics? *Bull. Chem. Soc. Jpn* **96**(7), 607–613 (2023). <https://doi.org/10.1246/bcsj.20230075>
85. Y. Yamamoto, S. Kushida, D. Okada, O. Oki, H. Yamagishi, Hendra, *Bull. Chem. Soc. Jpn* **96**, 702 (2023)
86. J. Chen, A. Tsuchida, A.D. Malay, K. Tsuchiya, H. Masunaga, Y. Tsuji, M. Kuzumoto, K. Urayama, H. Shintaku, K. Numata, *Nat. Commun.* **15**, 527 (2024)
87. Y. Honda, S. Nagao, H. Kinoh, X. Liu, N. Matsudaira, A. Dirisala, S. Nitta-Matsutomo, T. Nomoto, H. Hayashita-Kinoh, Y. Miura, T. Okada, N. Nishiyama, *ACS Nano* **19**, 7690 (2025)
88. T. Kitao, *Bull. Chem. Soc. Jpn* **97**, uoae103 (2024)
89. K. Sugamata, S. Kobayashi, A. Shirai, N. Amanokura, M. Minoru, *Bull. Chem. Soc. Jpn* **97**, uoae017 (2024)
90. R. Rani, T. Ueda, K. Saeki, K. Toda, S. Ohira, *Bull. Chem. Soc. Jpn* **97**, uoae113 (2024)
91. M. Wakizaka, M. Yamashita, *Chem. Phys. Rev.* **6**, 011301 (2025)
92. D. Jiang, X. Xu, Y. Bando, S.M. Alshehri, M. Eguchi, T. Asahi, Y. Yamauchi, *Bull. Chem. Soc. Jpn* **97**, uoae074 (2024)
93. T. Irie, S. Das, Q. Fang, Y. Negishi, *J. Am. Chem. Soc.* **147**, 1367 (2025)
94. E. De Bolòs, S. Bera, K. Strutyński, A.A. Bardin, R.W. Lodge, N.M. Padial, A. Saeki, C. Marti-Gastaldò, A.N. Khlobystov, B.L. Nannenga, M. Melle-Franco, A. Mateo-Alonso, *J. Am. Chem. Soc.* **147**, 2579 (2025)
95. S. Zhao, L. Dai, Z. Mai, B. Li, P. Zhang, M. Zhang, A. Matsuoka, K. Guan, R. Takagi, H. Matsuyama, *Adv. Sci.* **12**, 2500255 (2025)
96. F.-S. Xiao, L. Wang, C. Yin, K. Lin, Y. Di, J. Li, R. Xu, D.S. Su, R. Schlögl, T. Yokoi, T. Tatsumi, *Angew. Chem. Int. Ed.* **45**, 3090 (2006)
97. H. Matsune, R. Ikemizu, K. Shiomori, E. Muraoka, T. Yamamoto, M. Kishida, Colloidal trehalose nanoparticles: sacrifice templates for hollow silica nanospheres. *Bull. Chem. Soc. Jpn* **96**(8), 813–815 (2023). <https://doi.org/10.1246/bcsj.20230097>
98. S. Mohanan, C.I. Sathish, T.J. Adams, S. Kan, M. Liang, A. Vinu, A dual protective drug delivery system based on lipid coated core-shell mesoporous silica for efficient delivery of Cabazitaxel to prostate cancer cells. *Bull. Chem. Soc. Jpn* **96**(10), 1188–1195 (2023). <https://doi.org/10.1246/bcsj.20230167>
99. K.F. Vejchakul, M. Ogawa, Template syntheses of anatase nanoparticles using a nanoporous polyimide membrane: implications for deposition of platinum for photocatalytic H₂ evolution. *ACS Appl. Nano Mater.* **8**(7), 3402–3412 (2025). <https://doi.org/10.1021/acsnm.4c06376>
100. K. Uosaki, Y. Sato, H. Kita, *Langmuir* **7**, 1510 (1991)
101. M. Zharnikov, Y. Shoji, T. Fukushima, *Acc. Chem. Res.* **58**, 312 (2025)

102. Y. Kajino, Y. Tanaka, Y. Aida, Y. Arima, K. Tamada, Transfer printing of perovskite nanocrystal self-assembled monolayers via controlled surface wettability. *Nanoscale* **17**(14), 8651–8659 (2025). <https://doi.org/10.1039/D4NR05088F>
103. T. Tsuji, Y. Machida, S. De Feyter, K. Tahara, Y. Tobe, Multiguest-induced structural switching in a self-assembled monolayer network at the liquid–solid interface. *J. Phys. Chem. C* **129**(16), 7894–7902 (2025). <https://doi.org/10.1021/acs.jpcc.4c08516>
104. O.N. Oliveira Jr., L. Caseli, K. Ariga, *Chem. Rev.* **122**, 6459 (2022)
105. S. Negi, M. Hamori, Y. Kubo, H. Kitagishi, K. Kano, Monolayer formation and chiral recognition of binaphthyl amphiphiles at the air–water interface. *Bull. Chem. Soc. Jpn* **96**(1), 48–56 (2023). <https://doi.org/10.1246/bcsj.20220286>
106. K. Ariga, *Chem. Mater.* **35**, 5233 (2023)
107. T. Seki, *Bull. Chem. Soc. Jpn* **97**, bcsj.20230219 (2024)
108. R. Terui, Y. Otsuki, Y. Shibasaki, A. Fujimori, *Bull. Chem. Soc. Jpn* **97**, uoae050 (2024)
109. G. Decher, *Science* **277**, 1232 (1997)
110. K. Ariga, Y. Lvov, G. Decher, *Phys. Chem. Chem. Phys.* **24**, 4097 (2022)
111. K. Ariga, J. Song, K. Kawakami, Layer-by-layer designer nanoarchitectonics for physical and chemical communications in functional materials. *Chem. Commun.* **60**(16), 2152–2167 (2024). <https://doi.org/10.1039/d3cc04952c>
112. R. Suzuki, K. Nakano, M. Miyasaka, K. Tajima, Vertical component distributions in organic solar cells controlled by photocross-linking and layer-by-layer deposition. *Small* **21**(25), 2411988 (2025). <https://doi.org/10.1002/smll.202411988>
113. R.P. Feynman, *Eng. Sci.* **23**, 22 (1960)
114. M. Roukes, Plenty of room, indeed. *Sci. Am.* **285**(3), 48–57 (2001). <https://doi.org/10.1038/scientificamerican0901-48>
115. K. Ariga, Nanoarchitectonics: what's coming next after nanotechnology? *Nanoscale Horiz.* **6**(5), 364–378 (2021). <https://doi.org/10.1039/D0NH00680G>
116. K. Ariga, Q. Ji, J.P. Hill, Y. Bando, M. Aono, Forming nanomaterials as layered functional structures toward materials nanoarchitectonics. *NPG Asia Mater.* **4**(5), e17 (2012). <https://doi.org/10.1038/am.2012.30>
117. K. Ariga, Q. Ji, W. Nakanishi, J.P. Hill, M. Aono, *Mater. Horiz.* **2**, 406 (2015)
118. K. Ariga, M. Nishikawa, T. Mori, J. Takeya, L.K. Shrestha, J.P. Hill, Self-assembly as a key player for materials nanoarchitectonics. *Sci. Technol. Adv. Mater.* **20**(1), 51–95 (2019). <https://doi.org/10.1080/14686996.2018.1553108>
119. K. Ariga, *ChemNanoMat* **9**, e202300120 (2023)
120. K. Ariga, *Beilstein J. Nanotechnol.* **14**, 434 (2023)
121. K. Ariga, J. Li, J. Fei, Q. Ji, J.P. Hill, Nanoarchitectonics for dynamic functional materials from atomic-/molecular-level manipulation to macroscopic action. *Adv. Mater.* **28**(6), 1251–1286 (2016). <https://doi.org/10.1002/adma.201502545>
122. K. Ariga, X. Jia, J. Song, J.P. Hill, D.T. Leong, Y. Jia, J. Li, *Angew. Chem. Int. Ed.* **59**, 15424 (2020)
123. A. Nayak, S. Unayama, S. Tai, T. Tsuruoka, R. Waser, M. Aono, I. Valov, T. Hasegawa, Nanoarchitectonics for controlling the number of dopant atoms in solid electrolyte nanodots. *Adv. Mater.* **30**(6), 1703261 (2018). <https://doi.org/10.1002/adma.201703261>
124. J.M. Giussi, M.L. Cortez, W.A. Marmisollé, O. Azzaron, *Chem. Soc. Rev.* **48**, 814 (2019)
125. M. Eguchi, A.S. Nugraha, A.E. Rowan, J. Shapter, Y. Yamachi, Adsorchromism: molecular nanoarchitectonics at 2D nanosheets—old chemistry for advanced chromism. *Adv. Sci.* **8**(14), 2100539 (2021). <https://doi.org/10.1002/advs.202100539>
126. J. Muñoz, M. Palacios-Corella, I.J. Gómez, L. Zajíčková, M. Pumera, Synthetic nanoarchitectonics of functional organic–inorganic 2D germanane heterostructures via click chemistry. *Adv. Mater.* **34**(45), 2206382 (2022). <https://doi.org/10.1002/adma.202206382>
127. R. Hikichi, Y. Tokura, Y. Igarashi, H. Imai, Y. Oaki, Fluorine-free substrate-independent superhydrophobic coatings by nanoarchitectonics of polydispersed 2D materials. *Bull. Chem. Soc. Jpn* **96**(8), 766–774 (2023). <https://doi.org/10.1246/bcsj.20230126>
128. J. Song, A. Jancik-Prochazkova, K. Kawakami, K. Ariga, *Chem. Sci.* **15**, 18715 (2024)
129. M. Komiyama, K. Yoshimoto, M. Sisido, K. Ariga, Chemistry can make strict and fuzzy controls for bio-systems: DNA nanoarchitectonics and cell-macromolecular nanoarchitectonics. *Bull. Chem. Soc. Jpn* **90**(9), 967–1004 (2017). <https://doi.org/10.1246/bcsj.20170156>
130. R. Chang, L. Zhao, R. Xing, J. Li, X. Yan, *Chem. Soc. Rev.* **52**, 2688 (2023)
131. J. Song, K. Kawakami, K. Ariga, *Adv. Colloid Interface Sci.* **339**, 103420 (2025)
132. A.H. Khan, S. Ghosh, B. Pradhan, A. Dalui, L.K. Shrestha, S. Acharya, K. Ariga, *Bull. Chem. Soc. Jpn.* **90**, 627 (2017)
133. J. Kim, J.H. Kim, K. Ariga, *Joule* **1**, 739 (2017)
134. G. Chen, S.K. Singh, K. Takeyasu, J.P. Hill, J. Nakamura, K. Ariga, *K. Sci. Technol. Adv. Mater.* **23**, 413 (2022)
135. G. Chen, T. Koide, J. Nakamura, K. Ariga, *Small Methods* **2025**, 2500069 (2025)
136. H. Ullah, T.S. Alomar, M. Tariq, N. AlMasoud, M.H. Bhatti, M. Ajmal, Z. Nazar, M. Nadeem, H.M. Asif, M. Sohail, Nanoarchitectonics of molybdenum rich crown shaped polyoxometalates based ionic liquids reinforced on magnetic nanoparticles for the removal of microplastics and heavy metals from water. *J. Environ. Chem. Eng.* **12**(6), 114257 (2024). <https://doi.org/10.1016/j.jece.2024.114257>
137. T. Yang, A.G. Skirtach, *Materials* **18**, 1167 (2025)
138. S. Jain, N. Dilbaghi, G. Marrazza, A.A. Hassan, A. Kaushik, K.-H. Kim, S. Kumar, Nanoarchitectonics in colloidal hydrogels: design and applications in the environmental and biomedical fields. *Adv. Colloid Interface Sci.* **342**, 103529 (2025). <https://doi.org/10.1016/j.cis.2025.103529>
139. L.X. Yip, J. Wang, Y. Xue, K. Xing, C. Sevensan, K. Ariga, D.T. Leong, Cell-derived nanomaterials for biomedical applications. *Sci. Technol. Adv. Mater.* **25**(1), 2315013 (2024). <https://doi.org/10.1080/14686996.2024.2315013>
140. J. Song, W. Lyu, K. Kawakami, K. Ariga, *Nanoscale* **16**, 13230 (2024)
141. S. Chintalapati, E. Miyako, Hybrid nanoarchitectonics with bacterial component-integrated graphene oxide for cancer photo-thermo-chemo-immunotherapy. *Carbon* **238**, 120252 (2025). <https://doi.org/10.1016/j.carbon.2025.120252>
142. R.B. Laughlin, D. Pines, The theory of everything. *Proc. Natl. Acad. Sci. U.S.A.* **97**(1), 28–31 (2000). <https://doi.org/10.1073/pnas.97.1.28>
143. K. Ariga, R. Fakhruddin, Materials nanoarchitectonics from atom to living cell: a method for everything. *Bull. Chem. Soc. Jpn* **95**(5), 774–795 (2022). <https://doi.org/10.1246/bcsj.20220071>
144. K. Ariga, *Bull. Chem. Soc. Jpn* **97**, uoad001 (2024)
145. K. Ariga, *Materials* **18**, 654 (2025)
146. J.V. Vaghiasya, C.C. Mayorga-Martinez, M. Pumera, Wearable sensors for telehealth based on emerging materials and nanoarchitectonics. *NPJ Flex. Electron.* **7**(1), 26 (2023). <https://doi.org/10.1038/s41528-023-00261-4>
147. J.D. Bhaliya, V.R. Shah, G. Patel, K. Deshmukh, *J. Inorg. Organomet. Polym. Mater.* **33**, 1453 (2023)
148. P. Huang, W. Wu, M. Li, Z. Li, L. Pan, T. Ahamad, S.M. Alshehri, Y. Bando, Y. Yamauchi, X. Xu, Metal-organic framework-based nanoarchitectonics: a promising material platform for electrochemical detection of organophosphorus pesticides. *Coord.*

- Chem. Rev. **501**, 215534 (2024). <https://doi.org/10.1016/j.ccr.2023.215534>
149. B. Zhai, R. Huang, J. Tang, M. Li, J. Yang, G. Wang, K. Liu, Y. Fang, Film nanoarchitectonics of pillar[5]arene for high-performance fluorescent sensing: a proof-of-concept study. *ACS Appl. Mater. Interfaces* **13**(45), 54561–54569 (2021). <https://doi.org/10.1021/acsami.1c16272>
150. G. Li, M. Chao, C. Zhang, H. Gao, X. Li, H. Ren, X. Wei, C. Peng, W. Ma, Z. Wang, Supraparticle nanoarchitectonics with bright gold nanoclusters induced by host–guest recognition for volatile amine and meat freshness detection. *ACS Appl. Nano Mater.* **8**(11), 5763–5774 (2025). <https://doi.org/10.1021/acsnm.5c00366>
151. S. Deshmukh, K. Ghosh, M. Pykal, M. Otyepka, M. Pumera, *ACS Nano* **17**, 20537 (2023)
152. U. Kumar, Y.-W. Yeh, Z.-Y. Deng, W.-M. Huang, C.-H. Wu, *ACS Sens.* **10**, 2019 (2025)
153. S. Perumal, R. Atchudan, K. Krukiewicz, A. Banaś, D.R. Kumar, H. Lee, W. Lee, Nanoarchitectonics of polyaniline-poly(vinyl pyrrolidone)-graphene composite for the electrochemical sensing of ciprofloxacin and uric acid. *J. Taiwan Inst. Chem. Eng.* **172**, 106103 (2025). <https://doi.org/10.1016/j.jtice.2025.106103>
154. Y. Yang, X. Du, D. Jiang, X. Shan, W. Wang, H. Shiigi, Z. Chen, Photo-assisted Zn-air battery promoted self-powered sensor for selective and sensitive detection of antioxidant gallic acid based on Z-scheme nanoarchitectonics with heterojunction AgBr/CuBi₂O₄. *Sens. Actuators B Chem.* **393**, 134302 (2023). <https://doi.org/10.1016/j.snb.2023.134302>
155. A. Ashok, T.-K. Nguyen, M. Barton, M. Leitch, M.K. Masud, H. Park, T.-A. Truong, Y.V. Kaneti, H.T. Ta, X. Li, K. Liang, T.N. Do, C.-H. Wang, N.-T. Nguyen, Y. Yamauchi, H.-P. Phan, *Small* **19**, 2204946 (2023)
156. H.-M. Deng, M.-J. Xiao, Y.-L. Yuan, R. Yuan, Y.-Q. Chai, Organic-inorganic cascade-sensitized nanoarchitectonics for photoelectrochemical detection of β 2-MG protein. *Sens. Actuators B Chem.* **398**, 134715 (2024). <https://doi.org/10.1016/j.snb.2023.134715>
157. H. Li, L. Han, Q. Li, H. Lai, P. Fernández-Trillo, L. Tian, F. He, *Macromol. Rapid Commun.* **43**, 2100690 (2022)
158. M. Pandeewar, S.P. Senanayak, T. Govindaraju, *ACS Appl. Mater. Interfaces* **8**, 30362 (2016)
159. X. Niu, R. Zhao, Y. Liu, M. Yuan, H. Zhao, H. Li, X. Yang, H. Xu, K. Wang, *J. Mater. Chem. A* **11**, 23376 (2023)
160. P. Jiang, Y. Bai, L. Yan, P. Feng, K. Huang, J. Chen, *Anal. Chem.* **95**, 7676 (2023)
161. J. Minato, K. Miyazawa, Solvated structure of C₆₀ nanowhiskers. *Carbon* **43**(14), 2837–2841 (2005). <https://doi.org/10.1016/j.carbon.2005.06.013>
162. K. Miyazawa, Synthesis and properties of fullerene nanowhiskers and fullerene nanotubes. *J. Nanosci. Nanotechnol.* **9**(1), 41 (2009). <https://doi.org/10.1166/jnn.2009.J013>
163. M. Sathish, K. Miyazawa, Size-tunable hexagonal fullerene (C₆₀) nanosheets at the liquid–liquid interface. *J. Am. Chem. Soc.* **129**(45), 13816 (2007). <https://doi.org/10.1021/ja076251q>
164. T. Wakahara, M. Sathish, K. Miyazawa, C. Hu, Y. Tateyama, Y. Nemoto, T. Sasaki, O. Ito, Preparation and optical properties of fullerene/ferrocene hybrid hexagonal nanosheets and large-scale production of fullerene hexagonal nanosheets. *J. Am. Chem. Soc.* **131**(29), 9940 (2009). <https://doi.org/10.1021/ja901032b>
165. C. Park, E. Yoon, M. Kawano, T. Joo, H.C. Choi, Self-crystallization of C₇₀ cubes and remarkable enhancement of photoluminescence. *Angew. Chem. Int. Ed.* **49**(50), 9670 (2010). <https://doi.org/10.1002/anie.201005076>
166. Y. Xu, X. Chen, F. Liu, X. Chen, J. Guo, S. Yang, Ultrasonication-switched formation of dice- and cubic-shaped fullerene crystals and their applications as catalyst supports for methanol oxidation. *Mater. Horiz.* **1**(4), 411 (2014). <https://doi.org/10.1039/c4mh00037d>
167. S. Maji, L.K. Shrestha, K. Ariga, Nanoarchitectonics for hierarchical fullerene nanomaterials. *Nanomaterials* **11**(8), 2146 (2021). <https://doi.org/10.3390/nano11082146>
168. G. Chen, F. Sciortino, K. Takeyasu, J. Nakamura, J.P. Hill, L.K. Shrestha, K. Ariga, Hollow spherical fullerene obtained by kinetically controlled liquid–liquid interfacial precipitation. *Chem. Asian J.* **17**(20), e202200756 (2022). <https://doi.org/10.1002/asia.202200756>
169. P. Bairi, K. Minami, W. Nakanishi, J.P. Hill, K. Ariga, L.K. Shrestha, Hierarchically structured fullerene C₇₀ cube for sensing volatile aromatic solvent vapors. *ACS Nano* **10**(7), 6631 (2016). <https://doi.org/10.1021/acsnano.6b01544>
170. C.-T. Hsieh, S.-h Hsu, S. Maji, M.K. Chahal, J. Song, J.P. Hill, K. Ariga, L.K. Shrestha, Post-assembly dimension-dependent face-selective etching of fullerene crystals. *Mater. Horiz.* **7**(3), 787 (2020). <https://doi.org/10.1039/C9MH01866B>
171. G. Chen, B.N. Bhadra, L. Sutrisno, L.K. Shrestha, K. Ariga, Fullerene rosette: two-dimensional interactive nanoarchitectonics and selective vapor sensing. *Int. J. Mol. Sci.* **23**(10), 5454 (2022). <https://doi.org/10.3390/ijms23105454>
172. J. Song, T. Murata, K.-C. Tsai, X. Jia, F. Sciortino, R. Ma, Y. Yamauchi, J.P. Hill, L.K. Shrestha, K. Ariga, Fullerene nanosheets: a bottom-up 2D material for single-carbon-atom-level molecular discrimination. *Adv. Mater. Interfaces* **9**(11), 2102241 (2022). <https://doi.org/10.1002/admi.202102241>
173. B.N. Bhadra, L.K. Shrestha, R. Ma, J.P. Hill, Y. Yamauchi, K. Ariga, Metal–organic framework on fullerene (MOFOF) as a hierarchical composite by the integration of coordination chemistry and supramolecular chemistry. *ACS Appl. Mater. Interfaces* **16**(31), 41363–41370 (2024). <https://doi.org/10.1021/acsami.4c09747>
174. P. Bairi, K. Minami, J.P. Hill, K. Ariga, L.K. Shrestha, *ACS Nano* **11**, 7790 (2017)
175. Q. Tang, S. Maji, B. Jiang, J. Sun, W. Zhao, J.P. Hill, K. Ariga, H. Fuchs, Q. Ji, L.K. Shrestha, *ACS Nano* **13**, 14005 (2019)
176. M. Ishii, Y. Yamashita, S. Watanabe, K. Ariga, J. Takeya, Doping of molecular semiconductors through proton-coupled electron transfer. *Nature* **622**(7982), 285–291 (2023). <https://doi.org/10.1038/s41586-023-06504-8>
177. Y. Usami, Y. Yamashita, T. Murata, T. Matsumoto, M. Ito, S. Watanabe, J. Takeya, Scalable fabrication of precise flexible strain sensors using organic semiconductor single crystals. *Sci. Technol. Adv. Mater.* **26**(1), 2451020 (2025). <https://doi.org/10.1080/14686996.2025.2451020>
178. S. Maji, J. Hynek, K. Nakada, A. Hori, K. Minami, J. Labuta, M.K. Chahal, D.T. Payne, G.J. Richards, L.K. Shrestha, K. Ariga, Y. Yamauchi, G. Yoshikawa, J.P. Hill, Molecular nanoarchitectonic sensing layer for analysis of volatile fatty acids in bioreactor headspaces using a nanomechanical sensor. *Adv. Mater. Technol.* **10**(17), e00294 (2025). <https://doi.org/10.1002/admt.202500294>
179. M. Nishikawa, T. Murata, S. Ishihara, K. Shiba, L.K. Shrestha, G. Yoshikawa, K. Minami, K. Ariga, Discrimination of methanol from ethanol in gasoline using a membrane-type surface stress sensor coated with copper(I) complex. *Bull. Chem. Soc. Jpn* **94**(2), 648–654 (2021). <https://doi.org/10.1246/bcsj.20200347>
180. T. Murata, K. Minami, T. Yamazaki, G. Yoshikawa, K. Ariga, Detection of trace amounts of water in organic solvents by DNA-based nanomechanical sensors. *Biosensors* **12**(12), 1103 (2022). <https://doi.org/10.3390/bios12121103>
181. T. Murata, K. Minami, T. Yamazaki, T. Sato, H. Koinuma, K. Ariga, N. Matsuki, Nanometer-flat DNA-featured thin films prepared via laser molecular beam deposition under high-vacuum for selective methanol sensing. *Bull. Chem. Soc. Jpn* **96**(1), 29–34 (2023). <https://doi.org/10.1246/bcsj.20220303>

182. M.B. Avinash, T. Govindaraju, *Nanoscale* **6**, 13348 (2014)
183. Q. Zou, K. Liu, M. Abbas, X. Yan, Peptide-modulated self-assembly of chromophores toward biomimetic light-harvesting nanoarchitectonics. *Adv. Mater.* **28**(6), 1031–1043 (2016). <https://doi.org/10.1002/adma.201502454>
184. A. Jancik-Prochazkova, K. Ariga, *Research* **8**, 0624 (2025)
185. A. Jancik-Prochazkova, K. Ariga, Single-atom nanoarchitectonics for robotics and other functions. *ACS Sustainable Chem. Eng.* **13**(19), 6900–6917 (2025). <https://doi.org/10.1021/acssuschemeng.5c02606>
186. W. Chaikittisilp, Y. Yamauchi, K. Ariga, Material evolution with nanotechnology, nanoarchitectonics, and materials informatics: what will be the next paradigm shift in nanoporous materials? *Adv. Mater.* **34**(7), 2107212 (2022). <https://doi.org/10.1002/adma.202107212>
187. B. Bouider, B.S. Bouakaz, S. Haffad, A. Berrayah, A. Maguerresse, Y. Grohens, A. Habi, *J. Inorg. Organomet. Polym. Mater.* **33**, 3689 (2023)
188. R.S. Alruwais, W.A. Adeosun, *J. Inorg. Organomet. Polym. Mater.* **34**, 14 (2024)
189. A.P.S. Raman, M. Aslam, C. Naina, A. Verma, P. AlFantazi, A. Jain, P. Prajapat, *Inorg. Organomet. Polym. Mater.* **34**, 5035 (2024)
190. K. Ariga, *J. Inorg. Organomet. Polym. Mater.* **34**, 2926 (2024)
191. H.T. Alanazi, *J. Inorg. Organomet. Polym. Mater.* **35**, 2274 (2025)

Publisher's Note Springer Nature remains neutral with regard to jurisdictional claims in published maps and institutional affiliations.